ChemPubSoc Europe

DOI: 10.1002/cmdc.201402431

The Discovery of a Highly Selective 5,6,7,8-Tetrahydrobenzo[4,5]thieno[2,3-*d*]pyrimidin-4(3*H*)-one SIRT2 Inhibitor that is Neuroprotective in an in vitro Parkinson's Disease Model

Paolo Di Fruscia,[a] Emmanouil Zacharioudakis,[a] Chang Liu,[a] Sébastien Moniot,[b] Sasiwan Laohasinnarong,[c] Mattaka Khongkow,[c] Ian F. Harrison,[d] Konstantina Koltsida,[a] Christopher R. Reynolds,[e] Karin Schmidtkunz,[f] Manfred Jung,[f] Kathryn L. Chapman,[g] Clemens Steegborn,[b] David T. Dexter,[d] Michael J. E. Sternberg,[e] Eric W.-F. Lam,[c] and Matthew J. Fuchter*[a]

Sirtuins, NAD^+-dependent histone deacetylases (HDACs), have recently emerged as potential therapeutic targets for the treatment of a variety of diseases. The discovery of potent and isoform-selective inhibitors of this enzyme family should provide chemical tools to help determine the roles of these targets and validate their therapeutic value. Herein, we report the discovery of a novel class of highly selective SIRT2 inhibitors, identified by pharmacophore screening. We report the identification and validation of 3-((2-methoxynaphthalen-1-yl)methyl)-7-((pyridin-3-ylmethyl)amino)-5,6,7,8-tetrahydrobenzo[4,5]thieno[2,3-*d*]pyrimidin-4(3*H*)-one (ICL-SIRT078), a substrate-competitive SIRT2 inhibitor with a K_i value of 0.62 ± 0.15 μM and more than 50-fold selectivity against SIRT1, 3 and 5. Treatment of MCF-7 breast cancer cells with ICL-SIRT078 results in hyperacetylation of α-tubulin, an established SIRT2 biomarker, at doses comparable with the biochemical IC_{50} data, while suppressing MCF-7 proliferation at higher concentrations. In concordance with the recent reports that suggest SIRT2 inhibition is a potential strategy for the treatment of Parkinson's disease, we find that compound ICL-SIRT078 has a significant neuroprotective effect in a lactacystin-induced model of Parkinsonian neuronal cell death in the N27 cell line. These results encourage further investigation into the effects of ICL-SIRT078, or an optimised derivative thereof, as a candidate neuroprotective agent in in vivo models of Parkinson's disease.

Introduction

To date, 18 different members of the histone deacetylase (HDAC) family have been identified in humans. Based on their sequence homology to yeast HDACs and mechanism of action, they have been grouped into two families: the "classical" and the "sirtuin" families, and four classes.[1–4] Sirtuins (silent information regulator 2-related proteins) or class III HDACs share high sequence identity with the yeast *Saccharomyces cerevisiae* protein Sir2 (silent information regulator 2), show no sequence resemblance to members of the "classical" family of HDACs and require NAD^+ as the cofactor to affect deacetylation. The sirtuin family is broadly conserved from bacteria to humans, and to date seven sirtuin isoforms, named SIRT1–7, have been identified in humans. All SIRT proteins contain a conserved catalytic core domain comprised of approximately 275 amino acid residues with variable N and C termini. The seven isozymes differ in their substrate specificity, biological functions and cellular localisation: SIRT1, 6 and 7 principally localise in the nucleus, however, SIRT1 has also been found in the cytoplasm; SIRT2 is predominantly a cytoplasmic protein, but shuttles to the nucleus during mitosis; SIRT3, 4 and 5 are mitochondrial enzymes.[4]

In addition to the NAD^+-dependent deacetylation of ε-amino-acetylated lysine residues of target proteins by SIRTs, several of these enzymes have been reported to mediate other transformations. For example, SIRT4 and 6 have been shown to catalyse the ADP-ribosylation of protein substrates, using NAD^+ as a donor molecule,[5,6] and SIRT5 has significant desuccinylase activity.[7,8] In addition, SIRT6 has been recently report-

[a] Dr. P. Di Fruscia, E. Zacharioudakis, C. Liu, K. Koltsida, Dr. M. J. Fuchter
Department of Chemistry, Imperial College London
St. Kensington Campus, London SW7 2AZ, (UK)
E-mail: m.fuchter@imperial.ac.uk

[b] Dr. S. Moniot, Prof. Dr. C. Steegborn
Department of Biochemistry, University of Bayreuth (Germany)

[c] S. Laohasinnarong, M. Khongkow, Prof. E. W.-F. Lam
Department of Surgery and Cancer, Imperial College London (UK)

[d] I. F. Harrison, Prof. D. T. Dexter
Centre for Neuroinflammation & Neurodegeneration
Division of Brain Sciences, Imperial College London (UK)

[e] Dr. C. R. Reynolds, Prof. M. J. E. Sternberg
Department of Life Sciences, Imperial College London (UK)

[f] K. Schmidtkunz, Prof. Dr. M. Jung
Institute of Pharmaceutical Sciences, Albert-Ludwigs University (Germany)

[g] Dr. K. L. Chapman
Domainex Ltd, 162 Cambridge Science Park, Cambridge CB4 0GH (UK)

Supporting information for this article is available on the WWW under http://dx.doi.org/10.1002/cmdc.201402431.

ed to preferentially remove long-chain fatty acyl groups, such as myristoyl, from target lysine residues,[9] and it has been demonstrated that several biologically relevant free fatty acids (FFAs), including myristic, oleic and linoleic acid, induce up to a 35-fold increase in the deacetylation efficiency of SIRT6.[10] Long-chain deacetylation could well be a general feature of other mammalian sirtuins, providing new opportunities to investigate additional physiological functions that have been little explored until now.

The most studied sirtuin isoforms are certainly SIRT1 and SIRT2, which have been found to deacetylate a wide range of histone and nonhistone proteins, therefore playing a fundamental role in several physiological and pathological pathways.[11–14] While SIRT2 has been shown to deacetylate histone H4/K16,[15] its substrates are predominantly nonhistone proteins. For example, it has been found to inhibit adipocyte differentiation by regulating FoxO1 acetylation status,[16] to deacetylate FoxO3a in response to oxidative stress and caloric restriction,[17] to deacetylate α-tubulin,[18] and, as we and others have previously shown, to play a role in p53 deacetylation.[19] SIRT2 is overexpressed during mitosis, affecting the cell cycle,[20,21] and its activity has been found to be deregulated in a variety of cancers,[22–24] metabolic[16,25] and neurological disorders.[25–28] The exact physiological role and involvement of SIRT2 in human disease is not fully understood however, and further investigation is needed. Potent and selective small-molecule SIRT2 modulators could be used as tools to investigate and define the biological roles of SIRT2 and potentially as candidate agents to treat SIRT2-dependent pathologies.

A variety of SIRT inhibitors, some with selectivity for SIRT2, have been discovered to date (Figure 1).[29] These include the physiological inhibitor nicotinamide (**1**),[30] the 2-hydroxy-naphthaldehyde derivatives sirtinol (**2**),[31] cambinol[32] and salermide (**3**),[33] AGK2 (**4**),[28,34] AK-7 (**5**)[35] and its analogous 3-(*N*-arylsulfamoyl)benzamide derivatives,[36] the natural dilactone tanikolide dimer (**6**),[37] splitomicin derivatives,[38,39] suramin,[40] NAD^+ derivatives,[41] 3′-phenethyloxy-2-anilinobenzamide analogues (**7**),[42] our previously identified 10,11-dihydro-5*H*-dibenz[*b*,*f*]azepine derivative **8**,[43] thieno[3,2-*d*]pyrimidine-6-carboxamides (**9**),[44] thioacetylated pseudopeptides,[45] and a variety of recently discovered inhibitors.[46–49] There are still a number of significant challenges in the development of SIRT inhibitors however. These include the pressing need for more potent inhibitors, with the majority of inhibitors exhibiting IC_{50} values in the high micromolar range, the need for more selective inhibitors against a given isoform, and the need for further mechanism of action studies to aid compound development.

Herein, we report the discovery of a novel class of sub-micromolar, isoform-selective SIRT2 inhibitors based on a 5,6,7,8-tetrahydrobenzo[4,5]thieno[2,3-*d*]pyrimidin-4(3*H*)-one scaffold. Enzymatic data, cellular effects, and docking studies are presented and discussed, alongside preliminary data that show that these compounds are neuroprotective in an in vitro Parkinson's disease model.

Results and Discussion

Building on our previous work in this area,[43] we have continued to pursue the discovery of novel and highly isoform-selective SIRT2 inhibitory scaffolds. To guide our efforts, we decided to employ an innovative computational approach: "Investigational Novel Drug Discovery by Example" (INDDEx).[50] INDDEx is a software package developed by Equinox Pharma that uses

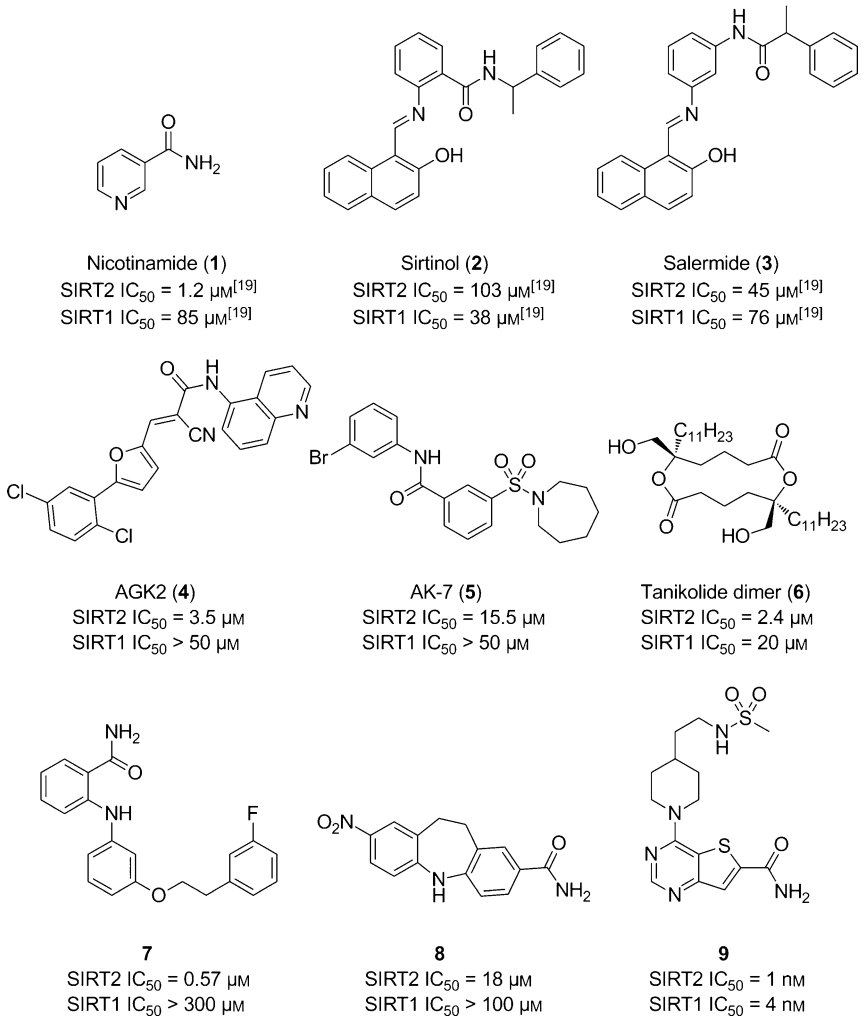

Figure 1. Molecular structures and SIRT1/2 inhibitory activities of several SIRT2 inhibitors reported in the literature.

a ligand-based virtual screening technology to build a predictive model of activity from training data of known active and inactive compounds for a pharmacological target. INDDEx uses a proprietary technology known as SVILP[51] to generate a pharmacophore model based on logical rules describing pairwise distances between fragments of a molecular substructure that are determined to affect the activity of the ligand. The logical rules can describe both positive and negative effects on activity. The rules in the pharmacophore model are weighted by a support vector machine (SVM) to give a quantitative structure–activity regression (QSAR) model, which can be applied to a compound structure to generate a predicted value of activity. In this study, INDDEx was used to generate a SIRT2 pharmacophore model from the chemical structures and measured activities of known active SIRT2 inhibitors (splitomicin-8c,[38] AGK2,[28,34] arylideneindolinone-9,[52] GW5074,[53] compound **8**,[43] cambinol[32]) and inactive SIRT2 inhibitors (our previously discovered inactive derivatives **8** containing the 10,11-dihydro-5*H*-dibenz[*b,f*]azepine scaffold).[43]

The INDDEx model was then used to predict and rank SIRT2 inhibition activity for all molecules in the purchasable subset of the ZINC 11 database, a free library containing over 25 million commercially available compounds in ready-to-dock, 3D formats.[54] The top 200 molecules that passed the Lipinski test, implemented in the ZINC 11 database ($150 \leq$ molecular weight ≤ 500, cLog$P \leq 5$, rotatable bonds ≤ 7, polar surface area ≤ 150 Å^2, hydrogen-bond donors ≤ 5 and hydrogen-bond acceptors ≤ 10) were selected.[55] In addition, the top-scoring 50 molecules were added to this set irrespective of whether they obey the Lipinski rules.

These two sets overlapped, sharing 14 molecules that passed the Lipinski test. Upon removing these duplicates, the resultant 236 molecules were further filtered by immediate commercial availability and cost ($\leq$100 U.S. dollars per sample). This gave 97 compounds that were subsequently docked at the active site of a SIRT2 enzyme crystal structure (PDB ID: 1J8F)[56] using GOLD version 5.0 as the docking software.[57] The top 40 molecules ranked by GOLD were carefully visually inspected and clustered into eight groups, based on their structural similarity and the single-linkage clustering method. The top-ranked compound of each group was purchased and screened for SIRT2 inhibitory activity. A diagram summarising the workflow of these efforts and details of the testing of the virtual screening hits are given in the Supporting Information.

This approach led us to the identification of compound **10** (ICL-SIRT078). Commercially obtained hit **10** (Figure 2) was found to have an IC_{50} value of 3.96 ± 0.87 μM, using a fluorimetric assay.[58] Interestingly, a commercially available structural analogue of this hit, compound **11**, was found to have comparably poor inhibition of SIRT2, giving only ≈22% inhibition at a 10 μM concentration. We felt this early structure–activity relationship was encouraging in terms of the development potential of this compound class as selective SIRT2 inhibitors.

Since the commercially obtained compounds were only quoted as being ≥90% pure, we first developed a synthetic route to hit **10** to allow confirmation of activity and preliminary analogue synthesis. Compound **10** was efficiently prepared, as a racemic mixture, in five steps and 14% overall yield from commercially available 1,4-cyclohexanedione monoethylene acetal (**12**) (Scheme 1). The synthesis commenced with formation of the 5,6,7,8-tetrahydrobenzo[4,5]thieno[2,3-*d*]pyrimidin-4(3*H*)-one tricyclic core structure, which was accomplished in

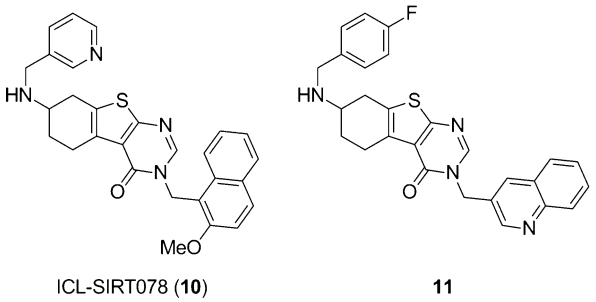

Figure 2. Molecular structures of ICL-SIRT078 (**10**) and compound **11**.

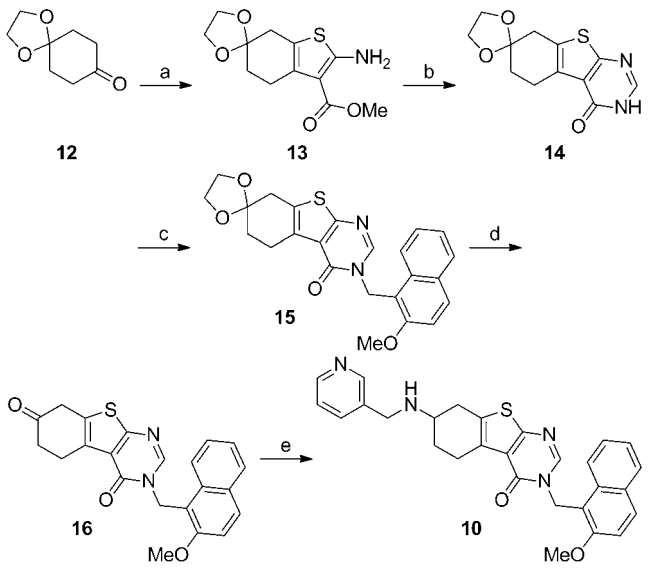

Scheme 1. Synthetic route to compound **10**. *Reagents and conditions*: a) Methyl 2-cyanoacetate, S_8, Et_2NH, EtOH, RT, 16 h; b) NH_2CHO, NH_4HCO_2, 150 °C (MW), 30 min; c) 1-(Chloromethyl)-2-methoxynaphthalene, Cs_2CO_3, DMF, RT, 16 h; d) CF_3CO_2H, H_2O, CH_2Cl_2, RT, 16 h; e) 3-picolylamine, $NaBH(OAc)_3$, AcOH, THF, RT, 16 h.

two steps. Condensation, via a Gewald reaction,[59] of the commercially available 1,4-cyclohexanedione monoethylene acetal (**12**) with methyl 2-cyanoacetate and elemental sulfur afforded 2-aminothiophene **13** in excellent yield (93%). Subsequent formation of the pyrimidone ring, through a microwave-assisted cyclisation in the presence of an excess of formamide and ammonium formate gave product **14**. Pyrimidone **14** was subsequently alkylated using 1-(chloromethyl)-2-methoxynaphthalene in the presence of caesium carbonate in *N*,*N*-dimethylformamide to give precursor **15** in good yield (73%). Removal of the acetal protecting group was achieved by treatment with trifluoroacetic acid in dichloromethane affording ketone **16** in high yield (95%), which was then successfully converted to the

desired hit compound **10** via a two-step, one-pot reductive amination employing 3-picolylamine, sodium triacetoxyborohydride and acetic acid in tetrahydrofuran.

Assessment of the effect of our re-synthesised material on SIRT2 enzymatic activity used a validated SIRT2 assay, based on a fluorogenic peptide substrate derived from p53 (see Experimental Section). This confirmed compound **10** to have a SIRT2 IC_{50} value of 1.45 ± 0.1 μM ($n = 3$). For this assay, suramin was used as a positive control and gave similar inhibitory activity to that observed previously.[40] DMSO was used as the negative control. It is worth noting that none of the compounds used in this study gave any signal interference in this assay format. Nonetheless, in light of the reported issues surrounding certain in vitro SIRT assays,[43,60] we sought to validate this result in alternative assay formats. Pleasingly, assessment in an enzyme-coupled SIRT-Glo assay gave a comparable, albeit more potent result, with a measured SIRT2 IC_{50} value of 0.17 ± 0.04 μM ($n = 3$) (Figure S1 in the Supporting Information). Furthermore, inhibition of SIRT2 activity using an α-tubulin peptide substrate (MPSD(ac)KTIG) was observed ($n = 2$) using mass spectrometry as a readout (Figure S2 in the Supporting Information).

We subsequently investigated the isoform selectivity of our hit compound. Compound **10** was assayed against SIRT1, 3 and 5 using the standard fluorogenic substrates. No inhibition against these isoforms was detected at concentrations up to 100 μM, revealing compound **10** to be highly selective (>65-fold) toward SIRT2 (Figure 3). Furthermore, the effect of our compound on SIRT1 activity was assessed in the enzyme-coupled SIRT-Glo assay, and also revealed our compound to be highly (≈50-fold) selective for SIRT2 (Figure S1 in the Supporting Information). In a final validation step, we checked our hit compound did not have any residual redox activity due to its 2-amino-3-carbonylthiophene substructure.[61] Compounds **10**, **22** and **23** (see below for analogues) were assessed for their ability to produce hydrogen peroxide in the presence of 1 mM dithiothreitol via redox cycling.[62] In this assay, the known SIRT1 inhibitor EX-527 was used as a negative control, whereas the redox-active NSC 663284 was used as a positive control[62] (Figure S3 in the Supporting Information). Compounds **10** and **22** were found to have no measureable redox activity at 100 μM. Compound **23** gave a low level of redox activity in this assay at 100 μM, but not at lower doses (data not shown). Thus it can be concluded that this common nonspecific inhibition mechanism is not operative for our specific compound series. It is also worth noting that we have observed no issue with the stability of compound **10** upon prolonged storage. A DMSO solution of compound **10** was stored under ambient conditions with no special precautions for approximately five weeks. The purity of the stored sample (by ^{1}H NMR and HPLC–MS analysis) was identical to the freshly prepared material.

Although the majority of published SIRT2 inhibitors are thought to bind to the NAD^+ binding pocket of the SIRT2 catalytic domain, competing with nicotinamide, in reality very little is understood about the exact binding site and mechanism of inhibition for most sirtuin modulators.[60] This situation is starting to be addressed however, combining in depth structural biology with suitable biochemical data.[63–65] We decided

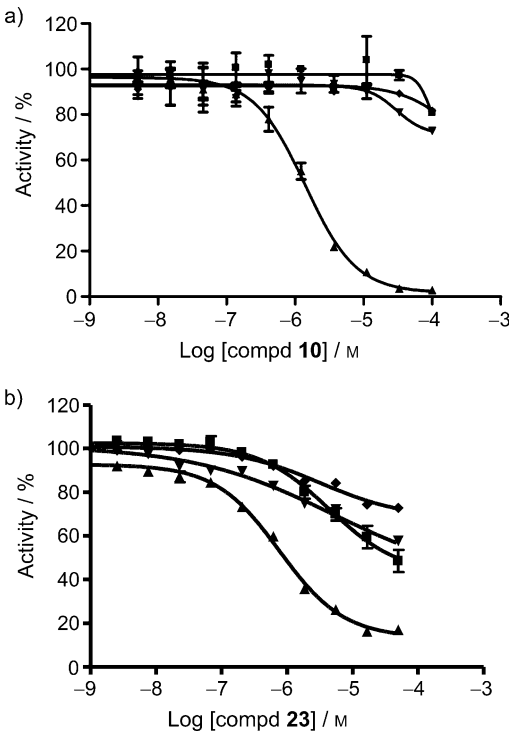

Figure 3. Concentration–inhibition curves for compounds a) **10** and b) **23** against SIRT1 (■), 2 (▲), 3 (▼) and 5 (◆). Errors bars represent the standard deviation, calculated from three replicates.

to conduct mechanistic studies to determine the mechanism of action for our hit compound. Testing SIRT2 activity at increasing peptide substrate concentrations in the presence of various concentrations of the more active enantiomer (see below) of the hit compound, (−)-**10**, revealed the activity pattern typical for competition (Figure 4), with an increase of the K_m value for the peptide in presence of the compound. The K_i value for this peptide-competitive SIRT2 inhibition by (−)-**10** was determined to be 0.62 ± 0.15 μM ($n = 2$). Analogous assays varying NAD^+ concentrations at different inhibitor levels re-

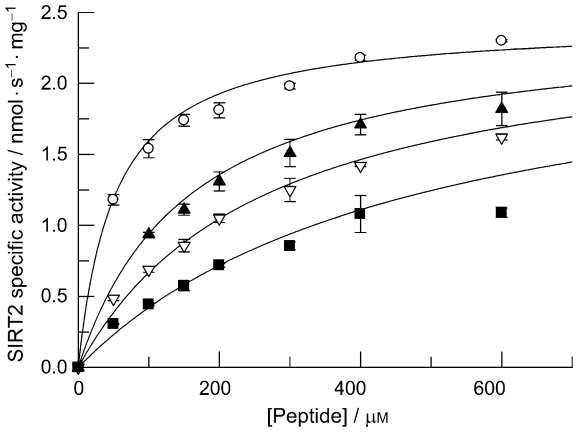

Figure 4. Competition assay for SIRT2 inhibition by (−)-**10**. SIRT2 activity against tubulin-K40 peptide measured at differing compound concentrations (0 μM: ○; 1.25 μM: ▲; 2.5 μM: ▽; 5 μM: ■) showed the pattern typical for competition, which was thus used as the model for fitting the data (lines).

sulted in an activity pattern consistent with noncompetitive inhibition, possibly with a small mixed component (Figure S4 in the Supporting Information). We thus conclude that compound **10** likely blocks the acetyl-lysine binding site of SIRT2, but shows no or only small overlap with the NAD^+ binding pocket.

With our developed synthetic route in hand, we prepared a number of analogues in order to establish initial structure–activity relationships. As before, the assessment of SIRT2 enzymatic activity employed a validated SIRT2 assay, where suramin[40] was used as a positive control ($IC_{50} = 15.5 \pm 0.4$) and vehicle (DMSO) was used as the negative control. Several analogues (**17**, **18** and **19**) were synthesised where the core framework of compound **10** had been truncated, and these analogues were tested against SIRT2 (Table 1). Clearly such dramatic changes were not tolerated, with all these simplified analogues significantly losing potency. We therefore sought to make more subtle changes, particularly in the western amino side chain. A variety of aliphatic and aromatic amines were investigated as alternative to 3-picolylamine (Table 1). Notably, the final reductive amination step in our synthetic route (Scheme 1) enabled the rapid preparation of such analogues.

Replacement of the pyridine ring of the picolyl side chain with a phenyl ring (compound **20**) resulted in an approximate 15-fold loss in potency against SIRT2. Further substituting the phenyl ring with an *ortho*-methyl substituent (compound **21**) gave a comparable potency to the unsubstituted phenyl ring. Replacing the pyridine ring with a thiophene heterocycle (compound **22**) gave a less dramatic loss in potency of approximately fivefold. Despite this trend, clearly certain aromatic substituents could compensate for the activity lost upon replacing the pyridine ring with a phenyl ring. The 3-fluorobenzyl and 3-methoxybenzyl analogues (compounds **23** and **24**, respectively) being only one- to threefold less potent than hit **10**. This could suggest that a suitably positioned polar functionality on the western side chain is important for SIRT2 activity. Interestingly, replacement of the aromatic ring with an aliphatic substituent (compound **25**) led to retention of SIRT2 activity and only an approximate fivefold drop in potency compared with hit molecule **10**. Compound **23** was selected as a representative analogue to study whether the isoform selectivity observed for hit compound **10** was general to this chemical series. Pleasingly, while less selective than hit **10**, compound **23** was still notably selective for SIRT2 (Figure 3), being 5.6-fold, 6.3-fold and 4.1-fold less potent against SIRT1, SIRT3 and SIRT5, respectively.

Since our hit compound **10** is chiral, we also resolved the enantiomers of **10** using preparative chiral HPLC and assessed the enantiopure material for SIRT2 activity (Table 1). The optical isomers of compound **10** differed in their SIRT2 IC_{50} value by approximately 14-fold. These data demonstrate that the absolute stereochemistry of compound **10** does have an effect on SIRT2 inhibitory activity, although both configurations at the chiral centre can be accommodated by SIRT2 upon binding. Unfortunately, based on the low amount of material available, we were unable to determine the absolute configuration of each enantiomer.

In an attempt to gain insights for compound refinement, hit **10** was docked into the active site of human SIRT2. Two protein structures were employed for this analysis. Initially, a human SIRT2 X-ray crystal structure (PDB ID: 1J8F)[56] was employed, however as this crystal structure is an apo-protein, we additionally performed docking studies on a ligand-bound structure. A human SIRT2 homology model was generated, predicted by the SWISS-MODEL server,[66] using the yeast Hst2 (yHst2) Sir2 X-ray crystal structure (PDB ID: 1Q17)[67] as a template. This yeast Hst2 structure is in ternary complex with 2′-*O*-acetyl ADP ribose and an acetylated histone H4 peptide. However, docking studies with the human SIRT2 X-ray crystal structure consistently gave higher-scoring binding modes, through the presence of stronger intermolecular interactions. The top-scoring poses of both optical isomers of compound **10** were predicted to bind to the acetylated-substrate pocket rather than the cofactor-binding cavity, in accordance with our mechanism of action studies (see above), displaying strong intermolecular interactions with the neighbouring active site amino acid residues and no clashes with the binding cleft. Furthermore, the three top-scoring poses (RMSD < 1) for each enantiomer gave comparable docking scores, which supports the biochemical data obtained.

Visual inspection of the top-ranked pose of compound **10**, at the active site of human SIRT2 X-ray structure, revealed a number of favourable potential intermolecular interactions (Figure 5). According to the docked pose, the heterotricyclic core scaffold is well accommodated into the acetylated-substrate binding tunnel, which allows the suitable positioning of the two opposite aromatic moieties, the pyridine and the naphthyl rings, in highly hydrophobic clefts. The pyridine ring, sandwiched between His 187 and Phe 119, forms π-stacking interactions with these residues, whereas the free amino NH group is hydrogen bonded to a tightly bound water molecule. On the other hand, the naphthyl moiety establishes several aromatic and hydrophobic interactions with Tyr 165, Phe 243, Met 247, Pro 268, Phe 269 and Leu 272 amino acid residues. All these favourable interactions could explain the high potency showed by compound **10**. To further validate the docking and biochemical findings, compounds **20** and **24** were also docked at the active site of human SIRT2 X-ray crystal structure. While displaying similar binding modes to hit **10**, the top-ranked docking solutions of both analogues showed lower scores, which correlates with the in vitro enzymatic data.

To rationalise the high SIRT2 isoform selectivity of compound **10**, as revealed by the biochemical assays, we decided to generate a superposition of the SIRT2 protein, bound to compound **10**, with the crystal structures of SIRT1 (PDB ID: 4IG9[68]), SIRT3 (PDB ID: 3GLS[69]) and SIRT5 (PDB ID: 2B4Y[70]). From this overlay, it is clear that hit **10** can no longer maintain the same binding mode within the catalytic site of other SIRT isozymes (Figure 5). Indeed, several clashes were observed between compound **10** and major loops in the active site of SIRT1, 3 and 5. In particular, the Leu 239 and Pro 268 residues of SIRT1, SIRT3 and SIRT5 were found to clash with the docked ligand. In SIRT2, these residues are further away from the docked ligand, due to increased space in the SIRT2 binding pocket.

Table 1. Molecular structures and SIRT2 biochemical inhibitory data for the synthesised compound library.

Compd	Structure	IC_{50} [μM][a]	Compd	Structure	IC_{50} [μM][a]
10	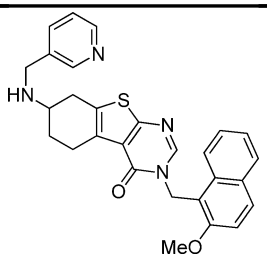	1.45 ± 0.1	**22**	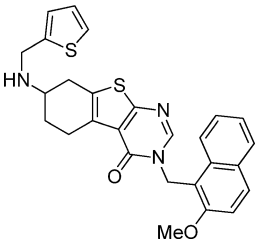	6.03 ± 2.25
17	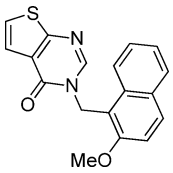	> 200	**23**	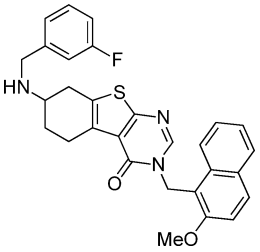	4.07 ± 0.87
18	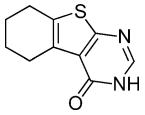	> 200	**24**	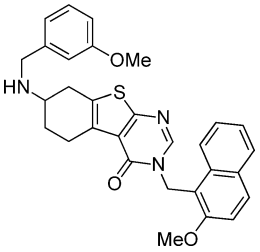	1.90 ± 0.09
19	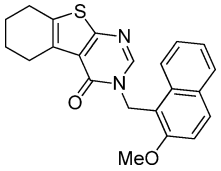	> 200	**25**	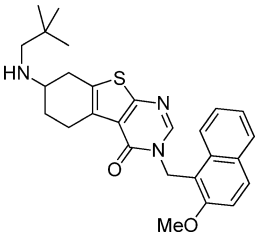	6.52 ± 0.01
20	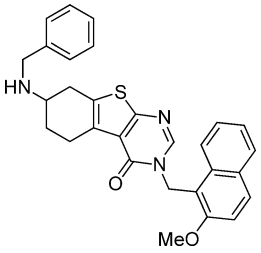	21.1 ± 4.3	(−)-**10**[b]	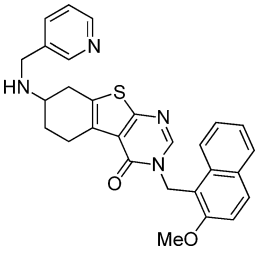	0.19 ± 0.02
21	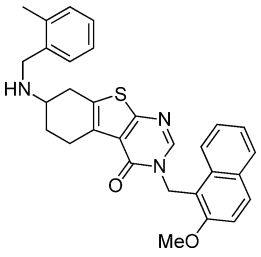	17.2 ± 5.5	(+)-**10**[b]	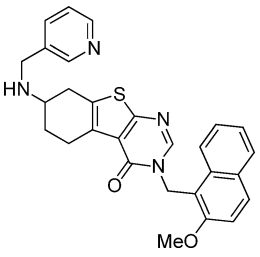	2.74 ± 0.19

[a] Errors represent the standard deviation, calculated from two replicates; [b] Absolute configuration not determined.

To gauge the cellular activity of **10**, the acetylation status of α-tubulin,[18] an established SIRT2 biomarker, was examined by Western blot analysis in the MCF-7 breast cancer cell line. We also included our previously published specific (albeit less potent) SIRT2 inhibitor, compound **8** (Figure 1), as a control. Increases in the acetyl-α-tubulin level were observed upon treatment with compound **10**. Relative to an untreated control, acetyl α-tubulin levels increase in a dose-dependent manner

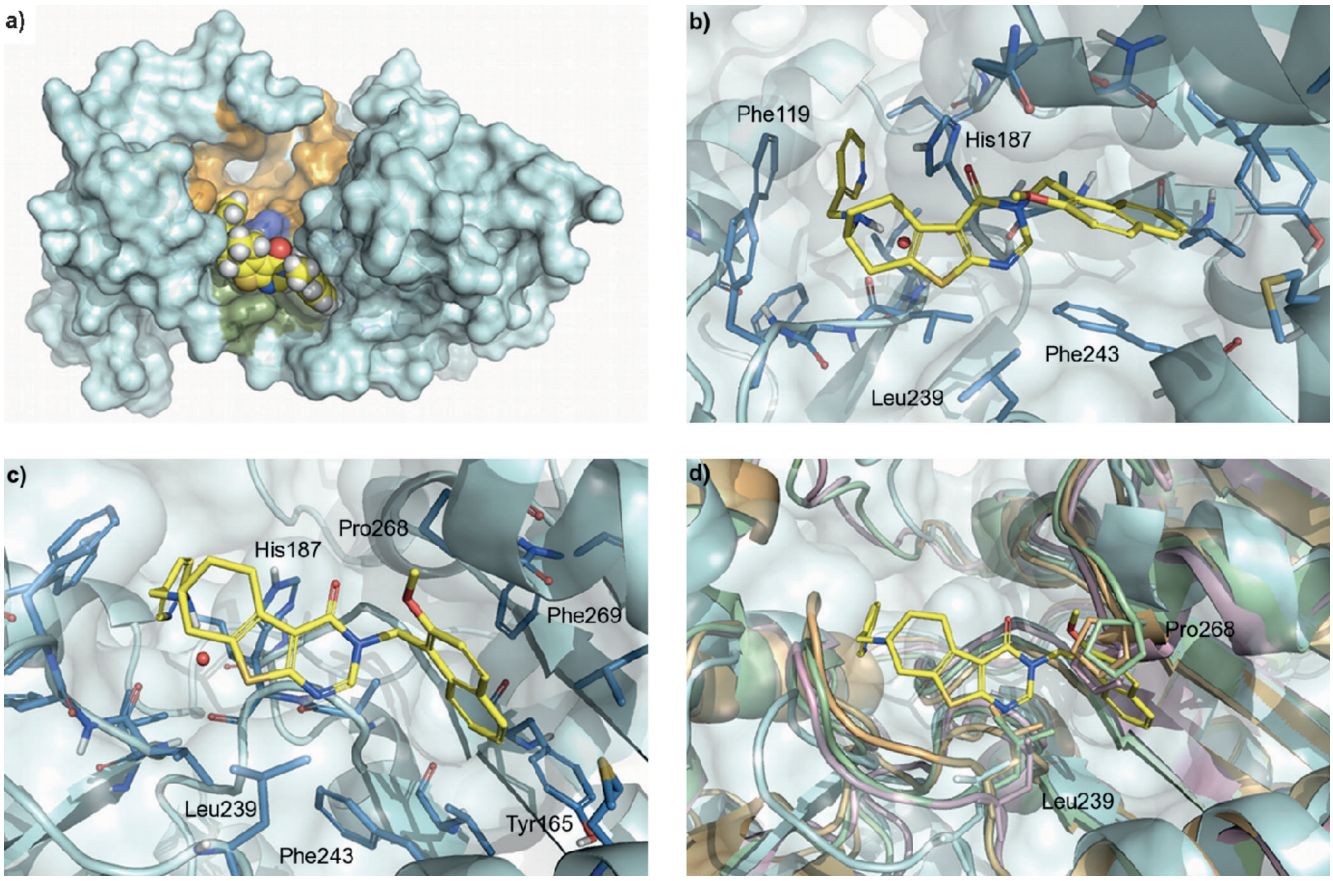

Figure 5. a) Predicted binding pose of **10** (space-filling representation) at the active site of human SIRT2 (molecular surface representation, PDB ID: 1J8F). NAD^+ binding site (orange surface), Ac-Lys pocket (green surface) and His 187 (blue surface) are displayed. b) and c) Close-up views of **10** (yellow stick representation) docked into the acetylated-substrate binding domain of SIRT2 (cyan ribbon and molecular surface representation). Active site residues (blue stick representation) and a key water molecule (red ball) are displayed. d) Rigid superposition of SIRT1 (pink ribbon representation, PDB ID: 4IG9), SIRT2 (cyan ribbon and molecular surface representation, PDB ID: 1J8F), SIRT3 (green ribbon representation, PDB ID: 3GLS) and SIRT5 (orange ribbon representation, PDB ID: 2B4Y) crystal structures. Compound **10** (yellow stick representation), docked into the acetylated-substrate binding domain of SIRT2, and critical active site residues (stick representation) are displayed.

from 0.5 μM, with the effect being largest at 1 μM. Beyond a dose of 2.5 μM, the acetyl tubulin level reaches a plateau. Higher concentrations were required to observe a comparable, albeit less dose-dependent response with compound **8** (Figure 6). The concentrations required to mediate these effects are in line with the different SIRT2 potencies of these two inhibitors: **10** SIRT2 $IC_{50} \approx 1$ μM (depending on assay); **8** SIRT2 $IC_{50} = 18$ μM.

Deacetylation of FOXO3a by SIRT2 has been shown to result in Skp2-mediated ubiquitination and degradation of FOXO3a,[71,72] suggesting inhibition of SIRT2 increases FOXO3a stability. Furthermore, we found that knockdown of SIRT2 is more effective in restoring the acetylation of FOXO3a compared with SIRT1 depletion (Figure S5 in the Supporting Information). The Western blot results revealed that both inhibitors **10** and **8** induce the accumulation of FOXO3a, but with **10** being more effective compared with the less potent inhibitor **8**. We have repeated these cellular experiments in four independent replicates and each time see a consistent response in terms of an increase in the levels of acetyl tubulin and FOXO3a.

Since there has been much interest in sirtuin inhibition as potential therapy for breast and lung cancers,[19,33,43] the effects of compound **10** on the proliferation of MCF-7 cells were also assessed.[19] Consistently, inhibitor **10** was more effective in arresting cell proliferation compared with **8**, as revealed by clonogenic assays (Figure 7). The dose responses observed correlate with the biochemical SIRT2 inhibitory potency for these compounds, suggesting this effect is target mediated. It should be noted that MCF7 cells have been previously shown to respond to SIRT2 inhibitors with a completely different scaffold.[38] Collectively, these data suggest that compound **10** is a SIRT2 inhibitor in cells and that it is even more potent than our previously reported specific SIRT2 inhibitor **8**.

Recently SIRT2 inhibition has emerged as a promising target for neurodegenerative diseases such as Parkinson's disease.[73] Notably, Outeiro et al.[34] showed that human neuroglioma H4 cells transfected with α-synuclein (αSyn), the altered protein associated with neurodegeneration in Parkinson's disease, can be rescued from αSyn-mediated toxicity dose dependently upon treatment with AGK2, a potent SIRT2 inhibitor. Furthermore, the authors demonstrated that feeding of AGK2 to

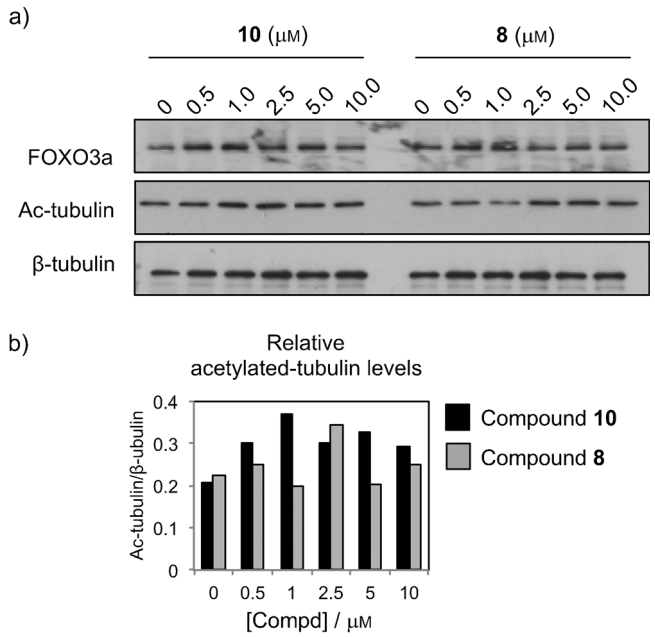

Figure 6. Compound **10** is more effective in inducing FOXO3a accumulation and tubulin acetylation compared with compound **8**. MCF-7 cells were treated with various doses of compounds **8** and **10** for 24 h. Cells were then harvested, and Western blot analysis was performed to determine the levels of FOXO3a, acetylated-α-tubulin and β-tubulin. a) Representative Western blot data are shown. b) Quantified acetylated-α-tubulin levels were normalised to β-tubulin. Quantification of protein expression was performed using ImageJ software (Image Processing and Analysis in Java).

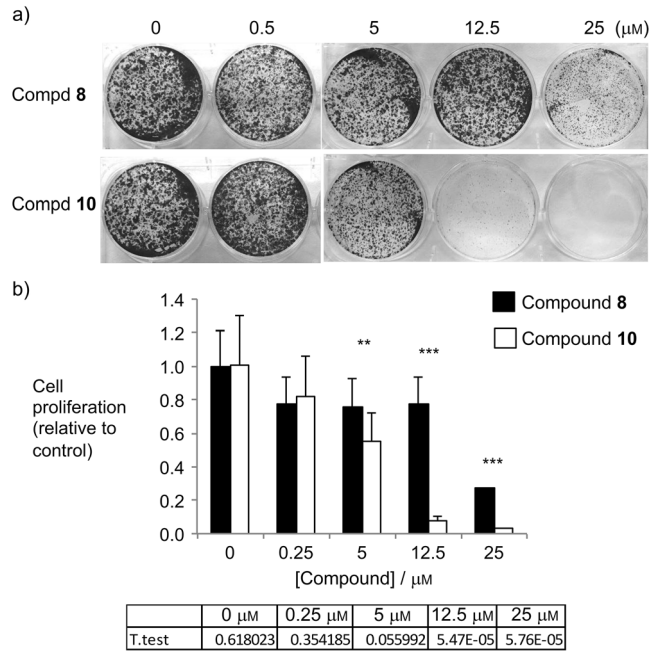

	0 μM	0.25 μM	5 μM	12.5 μM	25 μM
T.test	0.618023	0.354185	0.055992	5.47E-05	5.76E-05

Figure 7. Clonogenic assays were performed to assess the colony formation efficiency of MCF-7 cells following treatment with compounds **8** and **10**. A total of 2000 cells were seeded in six-well plates, treated with 0, 0.25, 5, 12.5 and 25 μM. a) Representative images of colonies after crystal violet staining. b) The result represents average of three independent experiments ± standard deviation. Statistical significance was determined by a Student's t-test: $^{*}p \leq 0.05$; $^{**}p \leq 0.01$; $^{***}p \leq 0.01$.

a transgenic *Drosophila* model of Parkinson's disease, in which αSyn is overexpressed in the fly brain, results in significant protection of dopaminergic dorsomedial neurons.[34] Therefore, we investigated the neuroprotective potential of compound **10** in an in vitro model of Parkinsonian neurodegeneration.

Since the discovery that the ubiquitin protesome system (UPS) becomes dysfunctional in dopaminergic nigrostriatal neurons in Parkinson's disease, irreversible UPS inhibitors such as lactacystin have been used in attempt to generate models of Parkinsonian cell death. Lactacystin covalently binds to catalytic subunits of the 20/26S proteasome, preventing accessibility of ubiquitinated proteins to the catalytic sites of UPS elements and therefore causes the cytoplasmic accumulation of unwanted proteins.[74,75] This translates to the formation of ubiquitin/αSyn immunopositive inclusions similar to those found in Parkinson's disease and in lactacystin-treated dopaminergic neurons, and subsequent neurodegeneration, both in vitro[75] and in vivo.[74,76–79] We therefore used lactacystin to model Parkinsonian neuronal cell death in the N27 mescencephalic dopaminergic cell line (Figure 8).[80]

In line with previous findings using a SIRT2 inhibitor,[34] here we observe that cultured N27 cells pretreated for 48 hours with compound **10** and subsequently treated with lactacystin display significantly greater neuronal survival than vehicle-treated controls, as ascertained from a combination of cell viability assays (Figure S6 in the Supporting Information). The 1.45 μM dose, at which a significant effect (≈23% neuroprotection) is observed, corresponds to the biochemical SIRT2 inhibitory potency and the cellular results obtained using MCF-7 cells (see above). At higher doses (10 μM and higher), neuro-

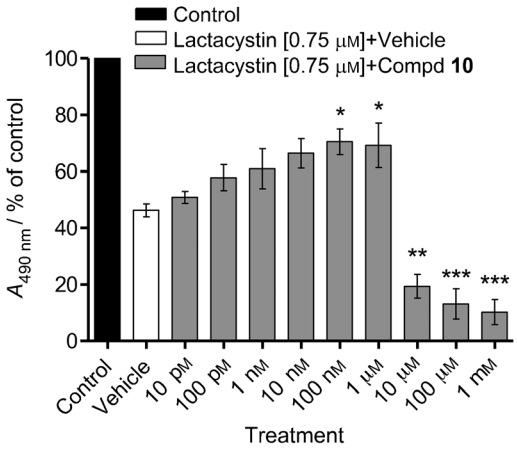

Figure 8. Compound **10**-mediated neuroprotection in an in vitro model of Parkinsonian cell death. Parkinsonian neurodegeneration was modelled in vitro using a cell line of rat mescenscephalic dopaminergic neurons treated with the irreversible proteasome inhibitor, lactacystin. Pretreatment for 48 h with **10** prior to treatment with lactacystin resulted in a dose-dependent increase in the absorbance reading at 490 nm wavelength in the MTS assay for cell viability, indicative of neuroprotection against lactacystin. This reached significance at 100 nM and 1 μM concentrations of **10**. Conversely pretreatment with higher concentrations of **10** resulted in significant neurotoxicity. Statistical significance ascertained from a one-way ANOVA with post-hoc Tukey's multiple comparisons test: $^{*}p < 0.05$, $^{**}p < 0.01$, $^{***}p < 0.001$, $n = 5$.

toxicity is observed. Such an effect is observed for all of the HDAC inhibitors and indeed, many of the drugs that are in clinical use are toxic at doses of over 10 μM for dopaminergic neurons. This could relate to off target effects of the compound at high concentrations.

Conclusions

Here we report the discovery of a novel class of sub-micromolar, isoform-selective SIRT2 inhibitors. In vitro biochemical assays revealed our best screening hit ICL-SIRT078 (**10**) to be a substrate-competitive SIRT2 inhibitor with a K_i value of 0.62 ± 0.15 μM, with high (>50-fold) selectivity over the SIRT1, 3 and 5 isoforms. Orthogonal assay formats and initial structure–activity relationship assessment were used to validate this hit. It is worth comparing the activity of hit compound **10** to the other reported SIRT2 probes (Figure 1). Commercially available compound **4** is one of the most used SIRT2 probes in the literature;[28,34] however, it is less potent (SIRT2 $IC_{50} = 3.5$ μM) and less selective than our hit. Furthermore, it is thought to have a co-factor (NAD^+)-competitive mechanism of action. Compound **7**[42] was reported recently and has a similar potency and selectivity profile to our hit, however, as for compound **4**, inhibitor **7** is thought to be co-factor competitive. The recently disclosed compounds developed by Sirtris (e.g., compound **9**)[44] have single-digit nanomolar potency for SIRT2, but are nonselective amongst the SIRT isoforms. Once again, compound **9** is thought to be co-factor (NAD^+)-competitive. Thus, the compound disclosed herein has an excellent potency and selectivity with respect to the state of the art, alongside a novel, substrate-competitive mechanism of action. We therefore feel it should make a highly useful probe of SIRT2 function. We note that a very recent report has emerged describing SIRT2 inhibitors discovered by a fragment-based screening approach.[81] While these inhibitors have a similar profile to those disclosed herein, they are structurally distinct, and therefore our compound offers a distinct chemotype to prosecute SIRT2 function.

In MCF-7 cells, upon treatment with compound **10**, we observed response of established SIRT2 biomarkers at comparable doses to the biochemical IC_{50} values. Furthermore, in line with previous findings using a SIRT2 inhibitor, we found compound **10** was neuroprotective in a Parkinsonian neuronal cell death model. Given the consistency of these findings with those previously published using compounds that have also shown efficacy in animal models of the disease (i.e., AGK2), our results encourage further investigation into the effects of compound **10**, or an optimised derivative thereof, as a candidate neuroprotective agent in in vivo models of Parkinson's disease. Indeed, further biological evaluation of hit molecule **10**, along with potency optimisation, are currently underway in our laboratories.

Experimental Section

Chemistry

Materials and methods: Chemical shifts (δ) are quoted in parts per million (ppm) and are referenced to a residual solvent peak: $CDCl_3$ ($\delta_H = 7.26$ ppm, $\delta_C = 77.0$ ppm), [D_6]DMSO ($\delta_H = 2.50$ ppm, $\delta_C = 39.5$ ppm). Coupling constants (J) are quoted in Hertz (Hz). Enantiomers of compound **10** were resolved by preparative HPLC, using a ChiralPak OJ-H 20×250 mm column and 35% 2-propanol containing 0.25% diethylamine (DEA) in CO_2 mobile phase (flow rate: 70 mL min^{-1}, detection: 220 nm). Purities of all assayed compounds were determined by combustion analysis or analytical HPLC and were found to be ≥95% pure unless otherwise specified. All manipulations of air- or moisture-sensitive materials were carried out in oven- or flame-dried glassware under an inert atmosphere of nitrogen or argon. Syringes, which were used to transfer reagents and solvents, were purged with nitrogen prior to use. Reaction solvents were distilled from CaH_2 (CH_2Cl_2), Na/Ph_2CO (THF) or obtained as anhydrous grade from commercial suppliers (DMF). All reagents were obtained from commercial suppliers and used without further purification unless indicated otherwise.

3-((2-Methoxynaphthalen-1-yl)methyl)-7-((pyridin-3-ylmethyl)-amino)-5,6,7,8-tetrahydrobenzo[4,5]thieno[2,3-*d*]pyrimidin-4(3*H*)-one (10): To a solution of **16** (70 mg, 0.18 mmol) in THF (5 mL) were added 3-picolylamine (18 μL, 0.18 mmol), $NaBH(OAc)_3$ (114 mg, 0.54 mmol) and AcOH (cat.). The resultant mixture was stirred at RT for 16 h. THF was evaporated in vacuo, and the residue partitioned between EtOAc (10 mL) and saturated aq Na_2CO_3 (10 mL). The organic layer was separated, washed with brine (10 mL), dried over $MgSO_4$, filtered, and the solvent evaporated in vacuo. The residue was purified by silica gel flash-column chromatography (CH_2Cl_2/MeOH, 9:1) to yield the title compound as a white solid (43 mg, 52%); mp: 138–140 °C; ^{1}H NMR (400 MHz, $CDCl_3$): $\delta = 1.74$–1.83 (m, 1H), 2.11–2.16 (m, 1H), 2.61–2.66 (m, 1H), 3.02–3.16 (m, 3H), 3.36 (dt, $J = 18.3$, 5.2 Hz, 1H), 3.92 (s, 2H), 4.02 (s, 3H), 5.66 (d, $J = 2.1$ Hz, 2H), 7.27 (d, $J = 4.8$ Hz, 1H), 7.33–7.38 (m, 2H), 7.49–7.53 (m, 1H), 7.71 (dt, $J = 7.6$, 2.2 Hz, 1H), 7.80 (d, $J = 8.4$ Hz, 1H), 7.84 (s, 1H), 7.92 (d, $J = 9.2$ Hz, 1H), 8.06 (d, $J = 8.8$ Hz, 1H), 8.51 (dd, $J = 3.2$, 1.6 Hz, 1H), 8.59 ppm (d, $J = 2.0$ Hz, 1H); ^{13}C NMR (100 MHz, $CDCl_3$): $\delta = 24.0$, 28.5, 32.1, 38.2, 48.5, 52.6, 56.3, 112.4, 115.5, 122.0, 122.9, 123.4, 124.0, 127.9, 128.5, 129.0, 131.1, 131.3, 131.4, 132.9, 135.6, 135.7, 145.6, 148.5, 149.6, 156.0, 158.1, 162.3 ppm; MS (ESI): $m/z = 483$ $[M+H]^+$; HRMS (FTMS): m/z $[M+H]^+$ calcd for $C_{28}H_{27}N_4O_2S$: 483.1855, found: 483.1846; Anal. calcd for $C_{28}H_{26}N_4O_2S$: C, 69.69; H, 5.43; N, 11.61, found: C, 69.60; H, 5.46; N, 11.58; HPLC: $t_R = 12.00$ min. The enantiomers of compound **10** were separated using preparative chiral HPLC. The enantiomers had the following optical rotations: (+)-**10** $[\alpha]_D^{29} = +7$ ($c = 0.14$, $CHCl_3$); (−)-**10** $[\alpha]_D^{29} = -7$ ($c = 0.14$, $CHCl_3$).

Methyl-2-amino-5,7-dihydro-4*H*-spiro[benzo[*b*]thiophene-6,2′-[1,3]dioxolane]-3-carboxylate (13): A solution of Et_2NH (882 μL, 8.55 mmol) in EtOH (3 mL) was added dropwise to a solution of **12** (4.0 g, 25.64 mmol), methyl 2-cyanoacetate (1.5 mL, 17.09 mmol) and elemental sulfur (547 mg, 17.09 mmol) in EtOH (5 mL). The resultant mixture was stirred at RT for 16 h and then cooled to −20 °C for 2 h. The product was collected by filtration in vacuo and triturated with hexane to give the title compound as a white solid (4.28 g, 93%); mp: 74–76 °C; ^{1}H NMR (400 MHz, $CDCl_3$): $\delta =$ 1.88 (t, $J = 6.6$ Hz, 2H), 2.72 (s, 2H), 2.90 (t, $J = 6.6$ Hz, 2H), 3.77 (s, 3H), 4.00 (s, 4H), 5.97 ppm (br s, 2H); ^{13}C NMR (100 MHz, $CDCl_3$): $\delta = 25.3$, 31.4, 34.8, 50.6, 64.6 (2C), 105.0, 108.2, 114.2, 131.4, 162.6,

166.3 ppm; MS (ESI): $m/z = 270$ $[M+H]^+$; HRMS (ESI): m/z $[M+H]^+$ calcd for $C_{12}H_{16}NO_4S$: 270.0800, found: 270.0802.

5,6-Dihydro-3*H*-spiro[benzo[4,5]thieno[2,3-*d*]pyrimidine-7,2′-[1,3]dioxolan]-4(8*H*)-one (14): A mixture of **13** (3.0 g, 11.15 mmol), excess NH_2CHO (20 mL) and NH_4HCO_2 (5.62 g, 89.20 mmol) was heated to 150 °C in a microwave reactor for 30 min. The mixture was cooled to RT, and H_2O (30 mL) was added. The resultant solid was collected by filtration in vacuo and triturated with H_2O to yield the title compound as an off-white solid (1.24 g, 42%); mp: 215–218 °C; ^{1}H NMR (400 MHz, [D$_6$]DMSO): $\delta = 1.87$ (t, $J = 6.2$ Hz, 2H), 2.92 (s, 2H), 3.00 (t, $J = 6.2$ Hz, 2H), 3.94 (s, 4H), 8.01 (s, 1H), 12.35 ppm (br s, 1H); ^{13}C NMR (100 MHz, [D$_6$]DMSO): $\delta = 24.3$, 31.0, 35.3, 64.4 (2C), 107.5, 122.5, 130.1, 130.2, 145.6, 158.1, 163.5 ppm; MS (ESI): $m/z = 265$ $[M+H]^+$; HRMS (ESI): m/z $[M+H]^+$ calcd for $C_{12}H_{13}N_2O_3S$: 265.0647, found: 265.0636; Anal. calcd for $C_{12}H_{12}N_2O_3S$: C, 54.53; H, 4.58; N, 10.60, found: C, 54.46; H, 4.48; N, 10.73.

3-((2-Methoxynaphthalen-1-yl)methyl)-5,6-dihydro-3*H*-spiro[benzo[4,5]thieno[2,3-*d*]pyrimidine-7,2′-[1,3]dioxolan]-4(8*H*)-one (15): To a solution of **14** (1.0 g, 3.79 mmol) in DMF (15 mL) were added 1-(chloromethyl)-2-methoxynaphthalene (1.17 g, 5.69 mmol) and Cs_2CO_3 (6.18 g, 18.95 mmol). The resultant mixture was stirred at RT for 16 h. The suspension was partitioned between EtOAc (100 mL) and H_2O (100 mL). The organic phase was separated and washed with brine (100 mL), dried over $MgSO_4$, filtered and the solvent evaporated in vacuo. The residue was purified by silica gel flash-column chromatography (hexanes/EtOAc, 7:3) to give the title compound as a white solid (1.2 g, 73%); mp: 162–164 °C; ^{1}H NMR (400 MHz, $CDCl_3$): $\delta = 2.01$ (t, $J = 6.4$ Hz, 2H), 2.97 (s, 2H), 3.33 (t, $J = 6.4$ Hz, 2H), 4.01 (s, 3H), 4.04 (s, 4H), 5.66 (s, 2H), 7.32–7.38 (m, 2H), 7.48–7.52 (m, 1H), 7.80 (d, $J = 8.1$ Hz, 1H), 7.83 (s, 1H), 7.91 (d, $J = 9.2$ Hz, 1H), 8.03 ppm (d, $J = 8.8$ Hz, 1H); ^{13}C NMR (100 MHz, $CDCl_3$): $\delta = 24.3$, 31.1, 35.6, 38.1, 56.3, 64.7 (2C), 107.9, 112.5, 115.6, 121.9, 122.9, 124.1, 127.9, 128.5, 129.1, 130.5, 130.6, 131.4, 132.9, 145.8, 156.0, 158.1, 162.6 ppm; MS (FTMS): $m/z = 435$ $[M+H]^+$; HRMS (FTMS): m/z $[M+H]^+$ calcd for $C_{24}H_{23}N_2O_4S$: 435.1379, found: 435.1374.

3-((2-Methoxynaphthalen-1-yl)methyl)-5,6-dihydrobenzo[4,5]-thieno[2,3-*d*]pyrimidine-4,7(3*H*,8*H*)-dione (16): To a solution of **15** (1.0 g, 2.30 mmol) in CH_2Cl_2 (20 mL) and H_2O (2 mL) was added CF_3CO_2H (5 mL). The resultant mixture was stirred at RT for 16 h. The solution was partitioned between CH_2Cl_2 (50 mL) and saturated aq $NaHCO_3$ (50 mL). The organic phase was separated and washed with brine (50 mL), dried over $MgSO_4$, filtered and the solvent evaporated in vacuo to give the title compound as a pale yellow solid (854 mg, 95%), which was used without further purification: mp: 216–219 °C; ^{1}H NMR (400 MHz, $CDCl_3$): $\delta = 2.75$ (t, $J = 6.8$ Hz, 2H), 3.57 (t, $J = 6.8$ Hz, 2H), 3.62 (s, 2H), 4.03 (s, 3H), 5.68 (s, 2H), 7.34–7.40 (m, 2H), 7.51–7.55 (m, 1H), 7.82 (d, $J = 8.1$ Hz, 1H), 7.90 (s, 1H), 7.94 (d, $J = 9.2$ Hz, 1H), 8.06 ppm (d, $J = 8.4$ Hz, 1H); ^{13}C NMR (100 MHz, $CDCl_3$): $\delta = 24.4$, 38.5, 38.6, 39.6, 56.4, 112.5, 115.3, 121.4, 122.8, 124.1, 127.9, 128.6, 129.1, 129.5, 131.2, 131.6, 132.9, 146.4, 156.1, 158.1, 163.2, 206.6 ppm; MS (FTMS): $m/z = 391$ $[M+H]^+$; HRMS (FTMS): m/z $[M+H]^+$ calcd for $C_{22}H_{19}N_2O_3S$: 391.1116, found: 391.1115.

3-((2-Methoxynaphthalen-1-yl)methyl)thieno[2,3-*d*]-pyrimidin-4-(3*H*)-one (17): Following the procedure described for the preparation of compound **15**, thieno[2,3-*d*]-pyrimidin-4(3*H*)-one (**26**) (150 mg, 0.98 mmol) was treated with 1-(chloromethyl)-2-methoxynaphthalene (305 mg, 1.47 mmol) and Cs_2CO_3 (1.6 g, 4.93 mmol) in DMF (5 mL) to give, after purification by silica gel flash-column chromatography (hexanes/EtOAc, 7:3), the title compound as a white solid (157 mg, 50%); mp: 155–157 °C; ^{1}H NMR (400 MHz, $CDCl_3$): $\delta = 4.03$ (s, 3H), 5.72 (s, 2H), 7.21 (d, $J = 6.1$ Hz, 1H), 7.33–7.39 (m, 3H), 7.54 (d, $J = 6.2$ Hz, 1H), 7.81 (d, $J = 8.3$ Hz, 1H), 7.92 (d, $J = 8.8$ Hz, 1H), 8.01 (s, 1H), 8.12 ppm (d, $J = 8.4$ Hz, 1H); ^{13}C NMR (100 MHz, $CDCl_3$): $\delta = 38.7$, 56.3, 112.4, 115.6, 122.4, 123.0, 123.4, 124.1, 124.2, 127.9, 128.6, 129.1, 131.5, 132.9, 146.4, 156.0, 158.0, 163.5 ppm; MS (ESI): $m/z = 323$ $[M+H]^+$; HRMS (ESI): m/z $[M+H]^+$ calcd for $C_{18}H_{15}N_2O_2S$: 323.0854, found: 323.0851; Anal. calcd for $C_{18}H_{14}N_2O_2S$: C, 67.06; H, 4.38; N, 8.69, found: C, 66.98; H, 4.44; N, 8.63.

5,6,7,8-Tetrahydrobenzo[4,5]thieno[2,3-*d*]pyrimidin-4(3*H*)-one (18): Following the procedure described for the preparation of compound **14**, methyl 2-amino-4,5,6,7-tetrahydrobenzo[*b*]thiophene-3-carboxylate (**27**) (500 mg, 2.36 mmol) was treated with excess NH_2CHO (3.8 mL) and NH_4HCO_2 (1.2 g, 18.95 mmol) to give the title compound as an orange solid (366 mg, 75%); mp: 226–228 °C; ^{1}H NMR (400 MHz, [D$_6$]DMSO): $\delta = 1.70$–1.81 (m, 4H), 2.72 (t, $J = 5.6$ Hz, 2H), 2.85 (t, $J = 6.1$ Hz, 2H), 7.98 (s, 1H), 12.27 ppm (br s, 1H); ^{13}C NMR (100 MHz, [D$_6$]DMSO): $\delta = 22.2$, 22.9, 24.8, 25.8, 123.1, 131.2, 132.5, 145.3, 158.1, 162.8 ppm; MS (ESI): $m/z = 207$ $[M+H]^+$; HRMS (ESI): m/z $[M+H]^+$ calcd for $C_{10}H_{11}N_2OS$: 207.0592, found: 207.0590; Anal. calcd for $C_{10}H_{10}N_2OS$: C, 58.23; H, 4.89; N, 13.58, found: C, 58.14; H, 4.73; N, 13.62.

3-((2-Methoxynaphthalen-1-yl)methyl)-5,6,7,8-tetrahydrobenzo-[4,5]thieno[2,3-*d*]pyrimidin-4(3*H*)-one (19): Following the procedure described for the preparation of compound **15**, **18** (100 mg, 0.48 mmol) was treated with 1-(chloromethyl)-2-methoxynaphthalene (150 mg, 0.72 mmol) and Cs_2CO_3 (790 mg, 2.42 mmol) in DMF (5 mL) to give, after purification by silica gel flash-column chromatography (hexanes/CH_2Cl_2, 1:9), the title compound as a white solid (58 mg, 32%); mp: 197–199 °C; ^{1}H NMR (400 MHz, $CDCl_3$): $\delta = 1.87$ (br s, 4H), 2.76 (br s, 2H), 3.12 (br s, 2H), 4.02 (s, 3H), 5.67 (s, 2H), 7.33–7.38 (m, 2H), 7.51 (t, $J = 7.2$ Hz, 1H), 7.80 (d, $J = 8.1$ Hz, 1H), 7.82 (s, 1H), 7.92 (d, $J = 9.2$ Hz, 1H), 8.06 ppm (d, $J = 8.4$ Hz, 1H); ^{13}C NMR (100 MHz, $CDCl_3$): $\delta = 22.3$, 22.9, 25.2, 25.7, 25.8, 38.1, 56.3, 112.5, 115.7, 123.0, 124.0. 127.9, 128.5, 129.1, 131.4, 131.7, 132.9, 133.7, 145.4, 156.1, 158.2, 161.9 ppm; MS (FTMS): $m/z = 377$ $[M+H]^+$; HRMS (FTMS): m/z $[M+H]^+$ calcd for $C_{22}H_{21}N_2O_2S$: 377.1324, found: 377.1323.

7-(Benzylamino)-3-((2-methoxynaphthalen-1-yl)methyl)-5,6,7,8-tetrahydrobenzo[4,5]thieno[2,3-*d*]pyrimidin-4(3*H*)-one (20): Following the procedure described for the preparation of compound **10**, **16** (50 mg, 0.13 mmol) was treated with benzylamine (16 μL, 0.15 mmol), $NaBH(OAc)_3$ (50 mg, 0.23 mmol) and AcOH (cat.) in THF (5 mL) to give, after purification by silica gel flash-column chromatography (CH_2Cl_2/MeOH, 9:1), the title compound as a dark grey solid (17 mg, 28%); mp: 168–170 °C; ^{1}H NMR (400 MHz, $CDCl_3$): $\delta = 1.84$–1.89 (m, 1H), 2.21–2.26 (m, 1H), 2.80–2.91 (m, 1H), 3.02–3.14 (m, 3H), 3.35 (dt, $J = 18.2$, 5.2 Hz, 1H), 3.95 (s, 2H), 4.02 (s, 3H), 5.68 (d, $J = 2.1$ Hz, 2H), 6.80–6.95 (m, 1H), 7.20 (d, $J = 7.6$ Hz, 3H), 7.25–7.35 (m, 3H), 7.51–7.55 (m, 2H), 7.80 (d, $J = 8.4$ Hz, 1H), 7.84 (s, 1H), 7.92 (d, $J = 9.2$ Hz, 1H), 8.06 ppm (d, $J = 8.8$ Hz, 1H); ^{13}C NMR (100 MHz, $CDCl_3$): $\delta = 24.3$, 28.7, 32.3, 38.2, 52.5, 55.5, 56.2, 112.5, 113.6, 115.8, 122.2, 122.8, 124.2, 127.7, 128.5, 129.1, 129.7, 131.3, 131.6, 131.7, 132.8, 141.9, 145.6, 156.1, 158.1, 159.9, 162.4 ppm; MS (ESI): $m/z = 482$ $[M+H]^+$; HRMS (EI): m/z $[M]^+$ calcd for $C_{29}H_{27}N_3O_2S$: 481.1824, found: 481.1898; HPLC: $t_R = 12.50$ min.

3-((2-Methoxynaphthalen-1-yl)methyl)-7-((2-methylbenzyl)amino)-5,6,7,8-tetrahydrobenzo[4,5]thieno[2,3-*d*]pyrimidin-4(3*H*)-

one (21): Following the procedure described for the preparation of compound **10**, **16** (50 mg, 0.13 mmol) was treated with *o*-tolylmethanamine (16 μL, 0.14 mmol), $NaBH(OAc)_3$ (50 mg, 0.23 mmol) and AcOH (cat.) in THF (5 mL) to give, after purification by silica gel flash-column chromatography (CH_2Cl_2/MeOH, 9:1), the title compound as a green solid (11 mg, 28%); mp: 164–166 °C; ^{1}H NMR (400 MHz, $CDCl_3$): δ = 1.84–1.89 (m, 1H), 2.21–2.26 (m, 1H), 2.40 (s, 3H), 2.80–288 (m, 1H), 3.02–3.14 (m, 3H), 3.35 (dt, J = 18.1, 5.2 Hz, 1H), 4.02 (s, 3H), 4.10 (s, 2H), 5.68 (d, J = 2.3 Hz, 2H), 6.84–6.94 (m, 1H), 7.18 (d, J = 7.6 Hz, 3H), 7.25–7.40 (m, 3H), 7.51–7.56 (m, 1H) 7.80 (d, J = 8.4 Hz, 1H), 7.84 (s, 1H), 7.92 (d, J = 9.2 Hz, 1H), 8.06 ppm (d, J = 8.8 Hz, 1H); ^{13}C NMR (100 MHz, $CDCl_3$): δ = 24.3, 28.7, 29.5, 30.8, 32.3, 38.2, 52.5, 55.2, 56.4, 112.5, 113.7, 115.7, 120.4, 122.1, 122.9, 124.1, 127.9, 128.6, 129.1, 129.5, 131.2, 131.5, 131.7, 132.9, 141.9, 145.6, 156.1, 158.1, 159.8, 162.3 ppm; MS (EI): m/z = 495 $[M]^+$; HRMS (EI): m/z $[M]^+$ calcd for $C_{30}H_{29}N_3O_2S$: 495.1980, found: 495.2013; HPLC: t_R = 12.54 min.

3-((2-Methoxynaphthalen-1-yl)methyl)-7-((thiophen-2-ylmethyl)amino)-5,6,7,8-tetrahydrobenzo[4,5]thieno[2,3-*d*]pyrimidin-4(3*H*)-one (22): Following the procedure described for the preparation of compound **10**, **16** (50 mg, 0.13 mmol) was treated with thiophen-2-ylmethanamine (16 μL, 0.14 mmol), $NaBH(OAc)_3$ (50 mg, 0.23 mmol) and AcOH (cat.) in THF (5 mL) to give, after purification by silica gel flash-column chromatography (CH_2Cl_2/MeOH, 9:1), the title compound as an off-white solid (13 mg, 20%); mp: 150–152 °C; ^{1}H NMR (400 MHz, $CDCl_3$): δ = 1.71–1.89 (m, 1H), 2.11–2.19 (m, 1H), 2.55–2.68 (m, 1H), 3.02–3.2 (m, 3H), 3.42 (dt, J = 18.3, 5.2 Hz, 1H), 4.02 (s, 3H), 4.23 (s, 2H), 5.68 (d, J = 2.1 Hz, 2H), 7.00 (s, J = 7.6 Hz, 2H), 7.20–7.30 (m, 1H), 7.32–7.45 (m, 2H), 7.49–7.53 (m, 1H), 7.80 (d, J = 8.4 Hz, 1H), 7.84 (s, 1H), 7.92 (d, J = 9.2 Hz, 1H), 8.06 ppm (d, J = 8.8 Hz, 1H); ^{13}C NMR (100 MHz, $CDCl_3$): δ = 23.3, 28.6, 32.1, 38.2, 45.6, 52.1, 56.4, 66.7, 112.5, 115.6, 122.1, 122.9, 124.1, 124.5, 124.9, 126.7, 127.8, 129.1, 131.2, 131.4, 131.6, 132.9, 144.1, 145.7, 156.1, 158.2, 162.4 ppm; MS (ESI): m/z = 488 $[M+H]^+$; HRMS (FTMS): m/z $[M+H]^+$ calcd for $C_{27}H_{26}N_3O_2S_2$: 488.1466, found: 488.1432; HPLC: t_R = 12.26 min.

7-((3-Fluorobenzyl)amino)-3-((2-methoxynaphthalen-1-yl)methyl)-5,6,7,8-tetrahydrobenzo[4,5]thieno[2,3-*d*]pyrimidin-4(3*H*)-one (23): Following the procedure described for the preparation of compound **10**, **16** (50 mg, 0.13 mmol) was treated with (3-fluorophenyl)methanamine (15 μL, 0.14 mmol), $NaBH(OAc)_3$ (50 mg, 0.23 mmol) and AcOH (cat.) in THF (5 mL) to give, after purification by silica gel flash-column chromatography (CH_2Cl_2/MeOH, 9:1), the title compound as a yellow solid (13 mg, 20%); mp: 156–159 °C; ^{1}H NMR (400 MHz, $CDCl_3$): δ = 1.74–1.89 (m, 1H), 2.11–2.16 (m, 1H), 2.60–2.72 (m, 1H), 3.02–3.14 (m, 3H), 3.39 (dt, J = 18.1, 5.2 Hz, 1H), 3.91 (s, 2H), 4.02 (s, 3H), 5.68 (d, J = 2.0 Hz, 2H), 6.87–6.94 (m, 1H), 7.18 (d, J = 7.6 Hz, 2H), 7.25–7.35 (m, 2H), 7.35–7.45 (m, 2H) 7.51–7.56 (m, 1H) 7.80 (d, J = 8.4 Hz, 1H), 7.84 (s, 1H), 7.92 (d, J = 9.2 Hz, 1H), 8.06 ppm (d, J = 8.8 Hz, 1H); ^{13}C NMR (100 MHz, $CDCl_3$): δ = 24.1, 28.5, 32.1, 38.2, 50.5, 52.5, 56.3, 112.1, 112.5, 112.9, 113.8, 114.0, 114.8, 115.0, 115.6, 123.6, 124.0, 127.9, 128.5, 129.1, 129.8, 129.9, 131.1, 131.4, 132.9, 145.6, 156.1, 158.1, 162.3 ppm; MS (ESI): m/z = 500 $[M+H]^+$; HRMS (EI): m/z $[M]^+$ calcd for $C_{29}H_{26}FN_3O_2S$: 499.1730, found: 499.1735; HPLC: t_R = 12.33 min.

7-((3-Methoxybenzyl)amino)-3-((2-methoxynaphthalen-1-yl)methyl)-5,6,7,8-tetrahydrobenzo[4,5]thieno[2,3-*d*]pyrimidin-4(3*H*)-one (24): Following the procedure described for the preparation of compound **10**, **16** (50 mg, 0.13 mmol) was treated with (3-methoxyphenyl)methanamine (19 μL, 0.14 mmol), $NaBH(OAc)_3$ (50 mg, 0.23 mmol) and AcOH (cat.) in THF (5 mL) to give, after purification by silica gel flash-column chromatography (CH_2Cl_2/MeOH, 9:1), the title compound as a pale green solid (10 mg, 15%); mp: 167–169 °C; ^{1}H NMR (400 MHz, $CDCl_3$): δ = 1.74–1.88 (m, 1H), 2.11–2.19 (m, 1H), 2.61–2.66 (m, 1H), 3.02–3.21 (m, 3H), 3.36 (dt, J = 18.0, 5.1 Hz, 1H), 3.80 (s, 3H), 3.90 (s, 2H), 4.05 (s, 3H), 5.66 (d, J = 2.1 Hz, 2H), 6.82 (d, J = 7.6 Hz, 2H), 6.91 (t, J = 7.3 Hz, 1H), 7.25 (d, J = 7.6 Hz, 1H), 7.49–7.53 (m, 2H), 7.55 (dt, J = 7.6, 2.1 Hz, 1H), 7.80 (d, J = 8.4 Hz, 1H), 7.84 (s, 1H), 7.92 (d, J = 9.2 Hz, 1H), 8.06 ppm (d, J = 8.8 Hz, 1H); ^{13}C NMR (100 MHz, $CDCl_3$): δ = 24.2, 28.7, 30.7, 32.1, 38.2, 52.5, 55.2, 56.4, 59.2, 112.5, 113.7, 115.7, 120.4, 122.2, 122.9, 124.1, 127.9, 128.6, 129.1, 129.5, 131.2, 131.5, 131.7, 132.9, 141.9, 145.6, 156.1, 158.1, 159.8, 162.3 ppm; MS (ESI): m/z = 512 $[M+H]^+$; HRMS (FTMS): m/z $[M+H]^+$ calcd for $C_{30}H_{30}N_3O_3S$: 512.2008, found: 512.2010; HPLC: t_R = 12.44 min.

3-((2-Methoxynaphthalen-1-yl)methyl)-7-(neopentylamino)-5,6,7,8-tetrahydrobenzo[4,5]thieno[2,3-*d*]pyrimidin-4(3*H*)-one (25): Following the procedure described for the preparation of compound **10**, **16** (50 mg, 0.13 mmol) was treated with neopentylamine (15 μL, 0.13 mmol), $NaBH(OAc)_3$ (50 mg, 0.23 mmol) and AcOH (cat.) in THF (5 mL) to give, after purification by silica gel flash-column chromatography (CH_2Cl_2/MeOH, 9:1), the title compound as a dark grey solid (10 mg, 15%); mp: 147–149 °C; ^{1}H NMR (400 MHz, $CDCl_3$): δ = 1.05 (s, 9H) 1.74–1.83 (m, 1H), 2.11–2.16 (m, 1H), 2.52 (s, 2H), 2.62–2.75 (m, 1H), 3.02–3.14 (m, 3H), 3.36 (dt, J = 18.3, 5.2 Hz, 1H), 4.02 (s, 3H), 5.68 (d, J = 2.1 Hz, 2H), 7.23 (d, J = 7.6 Hz, 1H), 7.49–7.53 (m, 1H), 7.71 (dt, J = 7.6, 2.1 Hz, 1H), 7.80 (d, J = 8.4 Hz, 1H), 7.84 (s, 1H), 7.92 (d, J = 9.2 Hz, 1H), 8.06 ppm (d, J = 8.8 Hz, 1H); ^{13}C NMR (100 MHz, $CDCl_3$): δ = 24.5, 27.7, 28.7, 31.4, 32.1, 38.3, 54.5, 56.4, 59.3, 112.5, 115.6, 122.1, 123.0, 124.1, 127.9, 128.6, 129.1, 131.1, 131.5, 131.8, 132.9, 145.6, 156.1, 158.1, 162.4 ppm; MS (ESI): m/z = 462 $[M+H]^+$; HRMS (FTMS): m/z $[M+H]^+$ calcd for $C_{27}H_{32}N_3O_2S$: 462.2215, found: 462.2223; HPLC: t_R = 12.18 min.

Thieno[2,3-*d*]pyrimidin-4(3*H*)-one (26): Following the procedure described for the preparation of compound **14**, methyl 2-aminothiophene-3-carboxylate (500 mg, 3.18 mmol) was treated with excess NH_2CHO (5 mL) and NH_4HCO_2 (1.6 g, 25.47 mmol) to give the title compound as an orange solid (198 mg, 41%), which was used without further purification; mp: 195–197 °C; ^{1}H NMR (400 MHz, [D$_6$]DMSO): δ = 7.39 (d, J = 6.2 Hz, 1H), 7.57 (d, J = 6.2 Hz, 1H), 8.12 (s, 1H), 12.46 ppm (br s, 1H); ^{13}C NMR (100 MHz, [D$_6$]DMSO): δ = 122.0, 124.2, 125.0, 146.0, 157.9, 164.7 ppm; MS (ESI): m/z = 153 $[M+H]^+$; HRMS (ESI): m/z $[M+H]^+$ calcd for $C_6H_5N_2OS$: 153.0123, found: 153.0156.

Methyl 2-amino-4,5,6,7-tetrahydrobenzo[*b*]thiophene-3-carboxylate (27): Following the procedure described for the preparation of compound **13**, cyclohexanone (1.6 mL, 15.18 mmol) was treated with methyl 2-cyanoacetate (888 μL, 10.10 mmol), elemental sulfur (322 mg, 10.10 mmol) and Et_2NH (520 μL, 5.05 mmol) in EtOH (3 mL) to give the title compound as a yellow solid (1.0 g, 50%), which was used without further purification; mp: 104–106 °C; ^{1}H NMR (400 MHz, $CDCl_3$): δ = 1.69–1.80 (m, 4H), 2.47–2.50 (m, 2H), 2.66–2.69 (m, 2H), 3.78 (s, 3H), 5.93 ppm (br s, 2H); ^{13}C NMR (100 MHz, $CDCl_3$): δ = 22.7, 23.2, 24.5, 26.8, 50.5, 105.5, 117.6, 132.4, 161.7, 166.5 ppm; MS (ESI): m/z = 212 $[M+H]^+$; HRMS (ESI): m/z $[M+H]^+$ calcd for $C_{10}H_{14}NO_2S$: 212.0745, found: 212.0749; Anal. calcd for $C_{10}H_{13}NO_2S$: C, 56.85; H, 6.20; N, 6.63, found: C, 56.49; H, 6.10; N, 6.70.

Biological methods

SIRT enzymatic assays: In vitro SIRT assays were conducted by using the fluorogenic peptide substrate from p53 residues 379–382

RHKK(Ac)-AMC for SIRT1–3 and an Ac-Lys-succ-AMC for SIRT5. The assay buffer contained 50 mM Tris-HCl, pH 8.0, 137 mM NaCl, 2.7 mM KCl, 1 mM $MgCl_2$, 1 mg mL^{-1} bovine serum albumin and 1% DMSO. The protocol involveed a two-step procedure. The fluorogenic substrate with the acetylated lysine side chain was incubated with the SIRT enzyme to produce the deacetylated products, which were then digested in the second step by the addition of a developer to produce the fluorescent signal proportional to the amount of deacetylated substrates. Deacetylation of substrate peptides was used as a read out of the SIRT activity. All compounds were freshly prepared as 10 mM stock solutions in DMSO and serially diluted to the indicated concentration (Figure 3) in the reaction. All test compounds were preincubated with the human SIRTs for about 10 min before commencing the reaction through the addition of substrate. Fluorescence was read (λ_{ex}: 360 nm; λ_{em}: 460 nm) using the EnVision Multilabel Plate Reader (PerkinElmer). The percentages of enzyme activity (relative to DMSO controls) and IC_{50} values were calculated using the GraphPad Prism 4 program based on a sigmoidal dose–response equation. The number of replicates is stated in the corresponding text.

SIRT2 mechanism of action assays: Recombinant human SIRT2 (43-356) was expressed as a His-Sumo fusion protein in *E. coli* and purified by affinity chromatography (HisTrap, GE Healthcare; 50 mM Tris-HCl, pH 8.0, 500 mM NaCl, 5% glycerol). The His-Sumo tag was cleaved overnight at 4 °C using Sumo-protease (protein ratio 1:100) and removed through reverse-affinity chromatography. The protein was further purified through gel filtration (S200 16/60, GE Healthcare; 25 mM BisTris propane, pH 6.5, 150 mM NaCl, 1 mM tris(2-carboxyethyl)phosphine). The deacetylase assay was performed as described elsewhere.[82] Briefly, the reaction mix contained 0.8 μM SIRT2, constant 500 μM NAD^+ for peptide titrations (50–600 μM) and constant 250 μM α-tubulin peptide, MPSD(ac)KTIG (GL Biochem, Shangai, China) for NAD^+ titrations (50–600 μM). NAD^+ and peptide titrations were performed at 0, 1.25, 2.5, and 5 μM of compound **10** with constant 5% DMSO in 20 mM sodium phosphate buffer (pH 7.5). The reaction was started by adding SIRT2 and followed for 1 h at RT through the absorbance decay at 340 nm in a microplate spectrophotometer MQX200 (MWG-Biotech, Germany). The background signal was measured under similar conditions, omitting the substrate peptide from the reaction. Results shown are the average of at least two measurements, and kinetic parameters were determined using Grafit 7 (Erathicus Software, Horley, UK).

MCF-7 cell culture: Cells were grown as a monolayer in Dulbecco's modified Eagle medium supplemented with 10% foetal bovine serum, 100 μg mL^{-1} streptomycin and 100 U mL^{-1} penicillin. Cells were incubated at 37 °C in an atmosphere of 5% of CO_2.

Western blot analysis: Whole-cell lysates were obtained, and Western blot analysis performed as described elsewhere.[83] Whole-cell protein extracts (20–25 μg) were resolved on 8–15% sodium dodecyl sulfate–polyacrylamide gel electrophoresis (SDS–PAGE) gels, transferred onto Protran nitrocellulose membranes (PerkinElmer) and incubated with specific antibodies in 1:1000 dilution. Antibodies against FOXO3a (#2497) were purchased from Cell Signalling Technology (Hitchin, UK). Antibodies against acetylated tubulin [6-11B-1] antibody (ab24610) were from Abcam (Cambridge, UK), and β-tubulin (sc-53646) from (Santa Cruz Biotechnology, Autogen Bioclear, Wiltshire, UK).

Clonogenic assays: Cells were seeded into six-well plates. Cells were then treated with test compound and cultured up to 15 days until colony formation. Colonies were washed with phosphate buffered saline and fixed with 4% paraformaldehyde for 20 min at RT. Visible colonies consisting of at least 50 cells were stained with 0.5% crystal violet (Sigma) and left to air dry at RT for a few days. AcOH 33% (*v/v*) was then added to solubilise the bound crystal violet, and the optical density (OD) was then measured at 592 nm using a Sunrise microplate reader (Tecan Group Ltd, Männedorf, Switzerland).

Neuronal cell death model: An immortalised line of rat dopaminergic neurons, $1RB3A_{N27}$ (N27), was maintained in RPMI 1640 medium supplemented with 10% foetal calf serum, 2 mM L-glutamine, 50 U mL^{-1} penicillin and 50 μg mL^{-1} streptomycin (henceforth termed "complete medium") in a humidified incubator temperature controlled at 37 °C and with 5% CO_2 ventilation. Cells were seeded at 1×10^4 cells/well in 96-well plates and left for 24 h to re-adopt their natural morphology. After this time, cell culture medium was replaced with fresh complete medium, and cells were pretreated for 48 h with compound **10** at the indicated concentrations before addition of the irreversible proteasome inhibitor lactacystin (Enzo Life Sciences, UK) to give a final concentration of 0.75 μM, shown in preliminary experiments to result in ≈40–50% cell death in this cell line (data not shown). All cell treatments were run in triplicate. Cytotoxicity assays were performed 24 h later. For performing the MTS (3-(4,5-dimethylthiazol-2-yl)-5-(3-carboxymethoxyphenyl)-2-(4-sulfophenyl)-2*H*-tetrazolium, inner salt) assay, the CellTiter 96 AQ_{ueous} One Solution Cell Proliferation Assay Kit (Promega, USA) was used as per the manufacturer's instructions. For performing the neutral red assay, a previously published protocol was followed.[84] The neutral red assay was followed sequentially by determination of total protein content in the same well as an additional endpoint measure of cell viability using a variation of the Bradford assay.[85] All data are expressed as a percentage of control wells treated with complete medium alone for each repeat and presented as mean ± SEM ($n=5$). Statistical significance was tested using a one-way ANOVA with post-hoc Tukey's multiple comparisons test.

Acknowledgements

The authors gratefully acknowledge Cancer Research UK (grant C21484A6944 and A12011 to EWFL) and The Royal Thai Government (studentships to SL and MK) for their financial support. CR was supported by a Biotechnology & Biological Sciences Research Council (BBSRC) Case studentship (BB/D526410/1) with help from Equinox Pharma (London, UK). IFH was supported by a studentship from the Medical Research Council (MRC), UK. The authors would like to thank Dr. Sandeep Sundriyal (Imperial College London, UK) for additional help with compound characterisation. MJ thanks the Deutsche Forschungsgemeinschaft (DFG) for funding (Ju295/8-1).

Keywords: acetylation · histone deacetylases (HDACs) · Parkinson's disease · SIRT · sirtuins

[1] I. V. Gregoretti, Y. M. Lee, H. V. Goodson, *J. Mol. Biol.* **2004**, *338*, 17–31.
[2] A. J. de Ruijter, A. H. van Gennip, H. N. Caron, S. Kemp, A. B. van Kuilenburg, *Biochem. J.* **2003**, *370*, 737–749.
[3] A. A. Sauve, C. Wolberger, V. L. Schramm, J. D. Boeke, *Annu. Rev. Biochem.* **2006**, *75*, 435–465.
[4] T. Finkel, C. X. Deng, R. Mostoslavsky, *Nature* **2009**, *460*, 587–591.
[5] L. R. Saunders, E. Verdin, *Oncogene* **2007**, *26*, 5489–5504.

[6] G. Laurent, N. J. German, A. K. Saha, V. C. de Boer, M. Davies, T. R. Koves, N. Dephoure, F. Fischer, G. Boanca, B. Vaitheesvaran, S. B. Lovitch, A. H. Sharpe, I. J. Kurland, C. Steegborn, S. P. Gygi, D. M. Muoio, N. B. Ruderman, M. C. Haigis, *Mol. Cell* **2013**, *50*, 686 – 698.
[7] J. Du, Y. Zhou, X. Su, J. J. Yu, S. Khan, H. Jiang, J. Kim, J. Woo, J. H. Kim, B. H. Choi, B. He, W. Chen, S. Zhang, R. A. Cerione, J. Auwerx, Q. Hao, H. Lin, *Science* **2011**, *334*, 806 – 809.
[8] F. Fischer, M. Gertz, B. Suenkel, M. Lakshminarasimhan, M. Schutkowski, C. Steegborn, *PLoS One* **2012**, *7*, e45098.
[9] H. Jiang, S. Khan, Y. Wang, G. Charron, B. He, C. Sebastian, J. Du, R. Kim, E. Ge, R. Mostoslavsky, H. C. Hang, Q. Hao, H. Lin, *Nature* **2013**, *496*, 110 – 113.
[10] J. L. Feldman, J. Baeza, J. M. Denu, *J. Biol. Chem.* **2013**, *288*, 31350 – 31356.
[11] S. Michan, D. Sinclair, *Biochem. J.* **2007**, *404*, 1 – 13.
[12] J. C. Milne, J. M. Denu, *Curr. Opin. Chem. Biol.* **2008**, *12*, 11 – 17.
[13] D. M. Taylor, M. M. Maxwell, R. Luthi-Carter, A. G. Kazantsev, *Cell. Mol. Life Sci.* **2008**, *65*, 4000 – 4018.
[14] J. A. Baur, Z. Ungvari, R. K. Minor, D. G. Le Couteur, R. de Cabo, *Nat. Rev. Drug Discovery* **2012**, *11*, 443 – 461.
[15] A. Vaquero, M. B. Scher, D. H. Lee, A. Sutton, H. L. Cheng, F. W. Alt, L. Serrano, R. Sternglanz, D. Reinberg, *Genes Dev.* **2006**, *20*, 1256 – 1261.
[16] E. Jing, S. Gesta, C. R. Kahn, *Cell Metab.* **2007**, *6*, 105 – 114.
[17] F. Wang, M. Nguyen, F. X. Qin, Q. Tong, *Aging Cell* **2007**, *6*, 505 – 514.
[18] B. J. North, B. L. Marshall, M. T. Borra, J. M. Denu, E. Verdin, *Mol. Cell* **2003**, *11*, 437 – 444.
[19] B. Peck, C. Y. Chen, K. K. Ho, P. Di Fruscia, S. S. Myatt, R. C. Coombes, M. J. Fuchter, C. D. Hsiao, E. W. Lam, *Mol. Cancer Ther.* **2010**, *9*, 844 – 855.
[20] S. C. Dryden, F. A. Nahhas, J. E. Nowak, A. S. Goustin, M. A. Tainsky, *Mol. Cell. Biol.* **2003**, *23*, 3173 – 3185.
[21] T. Inoue, Y. Nakayama, H. Yamada, Y. C. Li, S. Yamaguchi, A. Kurimasa, M. Katoh, M. Oshimura, *Cell Cycle* **2009**, *8*, 1279 – 1291.
[22] Y. Zhang, Q. Au, M. Zhang, J. R. Barber, S. C. Ng, B. Zhang, *Biochem. Biophys. Res. Commun.* **2009**, *386*, 729 – 733.
[23] Y. Li, H. Matsumori, Y. Nakayama, M. Osaki, H. Kojima, A. Kurimasa, H. Ito, S. Mori, M. Katoh, M. Oshimura, T. Inoue, *Genes Cells* **2011**, *16*, 34 – 45.
[24] H. S. Kim, A. Vassilopoulos, R. H. Wang, T. Lahusen, Z. Xiao, X. Xu, C. Li, T. D. Veenstra, B. Li, H. Yu, J. Ji, X. W. Wang, S. H. Park, Y. I. Cha, D. Gius, C. X. Deng, *Cancer Cell* **2011**, *20*, 487 – 499.
[25] R. Luthi-Carter, D. M. Taylor, J. Pallos, E. Lambert, A. Amore, A. Parker, H. Moffitt, D. L. Smith, H. Runne, O. Gokce, A. Kuhn, Z. Xiang, M. M. Maxwell, S. A. Reeves, G. P. Bates, C. Neri, L. M. Thompson, J. L. Marsh, A. G. Kazantsev, *Proc. Natl. Acad. Sci. USA* **2010**, *107*, 7927 – 7932.
[26] B. Beirowski, J. Gustin, S. M. Armour, H. Yamamoto, A. Viader, B. J. North, S. Michan, R. H. Baloh, J. P. Golden, R. E. Schmidt, D. A. Sinclair, J. Auwerx, J. Milbrandt, *Proc. Natl. Acad. Sci. USA* **2011**, *108*, E952 – E961.
[27] K. Harting, B. Knoll, *Eur. J. Cell Biol.* **2010**, *89*, 262 – 269.
[28] A. L. Garske, B. C. Smith, J. M. Denu, *ACS Chem. Biol.* **2007**, *2*, 529 – 532.
[29] J. Schemies, U. Uciechowska, W. Sippl, M. Jung, *Med. Res. Rev.* **2010**, *30*, 861 – 889.
[30] J. L. Avalos, K. M. Bever, C. Wolberger, *Mol. Cell* **2005**, *17*, 855 – 868.
[31] C. M. Grozinger, E. D. Chao, H. E. Blackwell, S. L. Schreiber, *J. Biol. Chem.* **2001**, *276*, 38837 – 38843.
[32] B. Heltweg, T. Gatbonton, A. D. Schuler, J. Posakony, H. Li, S. Goehle, R. Kollipara, R. A. Depinho, Y. Gu, J. A. Simon, A. Bedalov, *Cancer Res.* **2006**, *66*, 4368 – 4377.
[33] E. Lara, A. Mai, V. Calvanese, L. Altucci, P. Lopez-Nieva, M. L. Martinez-Chantar, M. Varela-Rey, D. Rotili, A. Nebbioso, S. Ropero, G. Montoya, J. Oyarzabal, S. Velasco, M. Serrano, M. Witt, A. Villar-Garea, A. Imhof, J. M. Mato, M. Esteller, M. F. Fraga, *Oncogene* **2009**, *28*, 781 – 791.
[34] T. F. Outeiro, E. Kontopoulos, S. M. Altmann, I. Kufareva, K. E. Strathearn, A. M. Amore, C. B. Volk, M. M. Maxwell, J. C. Rochet, P. J. McLean, A. B. Young, R. Abagyan, M. B. Feany, B. T. Hyman, A. G. Kazantsev, *Science* **2007**, *317*, 516 – 519.
[35] D. M. Taylor, U. Balabadra, Z. Xiang, B. Woodman, S. Meade, A. Amore, M. M. Maxwell, S. Reeves, G. P. Bates, R. Luthi-Carter, P. A. Lowden, A. G. Kazantsev, *ACS Chem. Biol.* **2011**, *6*, 540 – 546.
[36] S. H. Choi, L. Quinti, A. G. Kazantsev, R. B. Silverman, *Bioorg. Med. Chem. Lett.* **2012**, *22*, 2789 – 2793.
[37] M. Gutiérrez, E. H. Andrianasolo, W. K. Shin, D. E. Goeger, A. Yokochi, J. Schemies, M. Jung, D. France, S. Cornell-Kennon, E. Lee, W. H. Gerwick, *J. Org. Chem.* **2009**, *74*, 5267 – 5275.
[38] R. C. Neugebauer, U. Uchiechowska, R. Meier, H. Hruby, E. Verdin, W. Sippl, M. Jung, *J. Med. Chem.* **2008**, *51*, 1203 – 1213.
[39] D. Rotili, V. Carafa, D. Tarantino, G. Botta, A. Nebbioso, L. Altucci, A. Mai, *Bioorg. Med. Chem.* **2011**, *19*, 3659 – 3668.
[40] J. Trapp, R. Meier, D. Hongwiset, M. U. Kassack, W. Sippl, M. Jung, *ChemMedChem* **2007**, *2*, 1419 – 1431.
[41] T. Pesnot, J. Kempter, J. Schemies, G. Pergolizzi, U. Uciechowska, T. Rumpf, W. Sippl, M. Jung, G. K. Wagner, *J. Med. Chem.* **2011**, *54*, 3492 – 3499.
[42] T. Suzuki, M. N. Khan, H. Sawada, E. Imai, Y. Itoh, K. Yamatsuta, N. Tokuda, J. Takeuchi, T. Seko, H. Nakagawa, N. Miyata, *J. Med. Chem.* **2012**, *55*, 5760 – 5773.
[43] P. Di Fruscia, K. K. Ho, S. Laohasinnarong, M. Khongkow, S. H. B. Kroll, S. A. Islam, M. J. E. Sternberg, K. Schmidtkunz, M. Jung, E. W.-F. Lam, M. J. Fuchter, *MedChemComm* **2012**, *3*, 373 – 378.
[44] J. S. Disch, G. Evindar, C. H. Chiu, C. A. Blum, H. Dai, L. Jin, E. Schuman, K. E. Lind, S. L. Belyanskaya, J. Deng, F. Coppo, L. Aquilani, T. L. Graybill, J. W. Cuozzo, S. Lavu, C. Mao, G. P. Vlasuk, R. B. Perni, *J. Med. Chem.* **2013**, *56*, 3666 – 3679.
[45] P. Mellini, T. Kokkola, T. Suuronen, H. S. Salo, L. Tolvanen, A. Mai, M. Lahtela-Kakkonen, E. M. Jarho, *J. Med. Chem.* **2013**, *56*, 6681 – 6695.
[46] P. R. Tatum, H. Sawada, Y. Ota, Y. Itoh, P. Zhan, N. Ieda, H. Nakagawa, N. Miyata, T. Suzuki, *Bioorg. Med. Chem. Lett.* **2014**, *24*, 1871 – 1874.
[47] M. A. Khanfar, L. Quinti, H. Wang, S. H. Choi, A. G. Kazantsev, R. B. Silverman, *Eur. J. Med. Chem.* **2014**, *76*, 414 – 426.
[48] G. Hoffmann, F. Breitenbucher, M. Schuler, A. E. Ehrenhofer-Murray, *J. Biol. Chem.* **2014**, *289*, 5208 – 5216.
[49] C. Schlicker, G. Boanca, M. Lakshminarasimhan, C. Steegborn, *Aging* **2011**, *3*, 852 – 872.
[50] C. R. Reynolds, A. C. Amini, S. H. Muggleton, M. J. Sternberg, *J. Phys. Chem. B* **2012**, *116*, 6732 – 6739.
[51] *"Support Vector Inductive Logic Programming"*, S. H. Muggleton, H. M. Lodhi, M. J. E. Sternberg, A. Amini, (Imperial Innovations Limited, London, UK), U.S. Patent US,8,126,823, **2012**.
[52] K. Huber, J. Schemies, U. Uciechowska, J. M. Wagner, T. Rumpf, F. Lewrick, R. Suss, W. Sippl, M. Jung, F. Bracher, *J. Med. Chem.* **2010**, *53*, 1383 – 1386.
[53] J. Trapp, A. Jochum, R. Meier, L. Saunders, B. Marshall, C. Kunick, E. Verdin, P. Goekjian, W. Sippl, M. Jung, *J. Med. Chem.* **2006**, *49*, 7307 – 7316.
[54] J. J. Irwin, T. Sterling, M. M. Mysinger, E. S. Bolstad, R. G. Coleman, *J. Chem. Inf. Model* **2012**, *52*, 1757 – 1768.
[55] C. A. Lipinski, *J. Pharmacol. Toxicol. Methods* **2000**, *44*, 235 – 249.
[56] M. S. Finnin, J. R. Donigian, N. P. Pavletich, *Nat. Struct. Biol.* **2001**, *8*, 621 – 625.
[57] G. Jones, P. Willett, R. C. Glen, A. R. Leach, R. Taylor, *J. Mol. Biol.* **1997**, *267*, 727 – 748.
[58] B. Heltweg, J. Trapp, M. Jung, *Methods* **2005**, *36*, 332 – 337.
[59] G. Revelant, S. Dunand, S. Hesse, G. Kirsch, *Synthesis* **2011**, 2935 – 2940.
[60] M. Schutkowski, F. Fischer, C. Roessler, C. Steegborn, *Expert Opin. Drug Discovery* **2014**, *9*, 183 – 199.
[61] J. B. Baell, G. A. Holloway, *J. Med. Chem.* **2010**, *53*, 2719 – 2740.
[62] P. A. Johnston, K. M. Soares, S. N. Shinde, C. A. Foster, T. Y. Shun, H. K. Takyi, P. Wipf, J. S. Lazo, *Assay Drug Dev. Technol.* **2008**, *6*, 505 – 518.
[63] G. T. Nguyen, S. Schaefer, M. Gertz, M. Weyand, C. Steegborn, *Acta Crystallogr. Sect. D* **2013**, *69*, 1423 – 1432.
[64] M. Gertz, F. Fischer, G. T. T. Nguyen, M. Lakshminarasimhan, M. Schutkowski, M. Weyand, C. Steegborn, *Proc. Natl. Acad. Sci. USA* **2013**, *110*, E2772 – E2781.
[65] G. T. Nguyen, M. Gertz, C. Steegborn, *Chem. Biol.* **2013**, *20*, 1375 – 1385.
[66] K. Arnold, L. Bordoli, J. Kopp, T. Schwede, *Bioinformatics* **2006**, *22*, 195 – 201.
[67] K. Zhao, X. Chai, R. Marmorstein, *Structure* **2003**, *11*, 1403 – 1411.
[68] A. M. Davenport, F. M. Huber, A. Hoelz, *J. Mol. Biol.* **2014**, *426*, 526 – 541.
[69] L. Jin, W. Wei, Y. Jiang, H. Peng, J. Cai, C. Mao, H. Dai, W. Choy, J. E. Bemis, M. R. Jirousek, J. C. Milne, C. H. Westphal, R. B. Perni, *J. Biol. Chem.* **2009**, *284*, 24394 – 24405.

[70] T. Antoshenko, J. R. Min, A. Schuetz, P. Loppnau, A. M. Edwards, C. H. Arrowsmith, A. Bochkarev, A. N. Plotnikov, unpublished crystal structure of human sirtuin homolog 5 in complex with NAD (PDB ID: 2B4Y).
[71] F. Wang, C. H. Chan, K. Chen, X. Guan, H. K. Lin, Q. Tong, *Oncogene* **2012**, *31*, 1546 – 1557.
[72] K. Bonezzi, D. Belotti, B. J. North, C. Ghilardi, P. Borsotti, A. Resovi, P. Ubezio, A. Riva, R. Giavazzi, E. Verdin, G. Taraboletti, *Neoplasia* **2012**, *14*, 846 – 854.
[73] I. F. Harrison, D. T. Dexter, *Pharmacol. Ther.* **2013**, *140*, 34 – 52.
[74] K. S. McNaught, L. M. Bjorklund, R. Belizaire, O. Isacson, P. Jenner, C. W. Olanow, *Neuroreport* **2002**, *13*, 1437 – 1441.
[75] K. S. McNaught, C. Mytilineou, R. Jnobaptiste, J. Yabut, P. Shashidharan, P. Jennert, C. W. Olanow, *J. Neurochem.* **2002**, *81*, 301 – 306.
[76] C. Niu, J. Mei, Q. Pan, X. Fu, *Stereot. Funct. Neuros.* **2009**, *87*, 69 – 81.
[77] A. C. Vernon, S. M. Johansson, M. M. Modo, *BMC Neurosci.* **2010**, *11*, 1 – 18.
[78] E. Lorenc-Koci, T. Lenda, L. Antkiewicz-Michaluk, J. Wardas, H. Domin, M. Smialowska, J. Konieczny, *Neurochem. Int.* **2011**, *58*, 839 – 849.
[79] I. S. Pienaar, I. F. Harrison, J. L. Elson, A. Bury, P. Woll, A. K. Simon, D. T. Dexter, *Brain Struct. Funct.* **2013**, DOI: 10.1007/s00429-013-0669-5.
[80] F. S. Adams, F. G. La Rosa, S. Kumar, J. Edwards-Prasad, S. Kentroti, A. Vernadakis, C. R. Freed, K. N. Prasad, *Neurochem. Res.* **1996**, *21*, 619 – 627.
[81] H. Cui, Z. Kamal, T. Ai, Y. Xu, S. S. More, D. J. Wilson, L. Chen, *J. Med. Chem.* **2014**, *57*, 8340 – 8357
[82] a) B. C. Smith, W. C. Hallows, J. M. Denu, *Anal. Biochem.* **2009**, *394*, 101 – 109; b) S. Moniot, M. Schutkowski, C. Steegborn, *J. Struct. Biol.* **2013**, *182*, 136 – 43.
[83] A. Essafi, A. R. Gomes, K. M. Pomeranz, A. K. Zwolinska, R. Varshochi, U. B. McGovern, E. W. Lam, *Methods Mol. Biol.* **2009**, *462*, 201 – 211.
[84] G. Repetto, A. del Peso, J. L. Zurita, *Nat. Protoc.* **2008**, *3*, 1125 – 1131.
[85] M. J. Arranz, M. F. Festing, *Toxicol. In Vitro* **1990**, *4*, 211 – 212.

Received: October 7, 2014
Published online on ■■ ■■, 0000

Hit discovery: Through ligand-based virtual screening validation, ICL-SIRT078, a cell-active substrate-competitive SIRT2 inhibitor with a K_i value of 0.62 ± 0.15 μM and more than 50-fold selectivity against SIRT1, 3 and 5 was identified. In addition, ICL-SIRT078 shows a significant neuroprotective effect in a lactacystin-induced model of Parkinsonian neuronal cell death in the N27 cell line. ICL-SIRT078, or an optimised derivative thereof, warrants further investigation as a neuroprotective agent in in vivo models of Parkinson's disease.

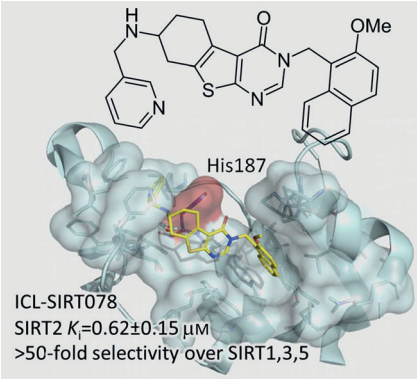

*P. Di Fruscia, E. Zacharioudakis, C. Liu, S. Moniot, S. Laohasinnarong, M. Khongkow, I. F. Harrison, K. Koltsida, C. R. Reynolds, K. Schmidtkunz, M. Jung, K. L. Chapman, C. Steegborn, D. T. Dexter, M. J. E. Sternberg, E. W.-F. Lam, M. J. Fuchter**

■■ – ■■

The Discovery of a Highly Selective 5,6,7,8-Tetrahydrobenzo[4,5]thieno[2,3-*d*]pyrimidin-4(3*H*)-one SIRT2 Inhibitor that is Neuroprotective in an in vitro Parkinson's Disease Model